

CERN-TH.7263/94.  
 LPTHE Orsay-94/49  
 HUTP-94/A015  
 HD-THEP-94-20  
 FTUAM-94/14  
 NSF-ITP-94-65  
 hep-ph/9406289

# Standard Model CP-violation and Baryon asymmetry

## Part II: Finite Temperature

M.B. Gavela<sup>a</sup>, P. Hernandez<sup>b</sup>, J. Orloff<sup>c</sup>, O.Pène<sup>d</sup>, C. Quimbay<sup>e</sup>.

<sup>a</sup> CERN, TH Division, CH-1211, Geneva 23, Switzerland

<sup>b</sup> Lyman lab., Harvard University, Cambridge, MA 02138<sup>1</sup>

<sup>c</sup> Institut für Theoretische Physik, Univ. Heidelberg

<sup>d</sup> LPTHE, F 91405 Orsay, France,<sup>2</sup>

<sup>e</sup> CERN, TH Division, CH-1211, Geneva 23, Switzerland<sup>3</sup>.

### Abstract

We consider the scattering of quasi-particles off the boundary created during a first order electroweak phase transition. Spatial coherence is lost due to the quasi-quark damping rate, and we show that reflection on the boundary is suppressed, even at tree-level. Simply on CP considerations, we argue against electroweak baryogenesis in the Standard Model via the charge transport mechanism. A CP asymmetry is produced in the reflection properties of quarks and antiquarks hitting the phase boundary. An effect is present at order  $\alpha_W^2$  in rate and a regular GIM behaviour is found, which can be expressed in terms of two unitarity triangles. A crucial role is played by the damping rate of quasi-particles in a hot plasma, which is a relevant scale together with  $M_W$  and the temperature. The effect is many orders of magnitude below what observation requires.

---

<sup>1</sup>Junior Fellow, Harvard Society of Fellows

<sup>2</sup>Laboratoire associé au Centre National de la Recherche Scientifique.

<sup>3</sup>On leave of absence from Dpto. de Física Teórica, Univ. Autónoma de Madrid, Cantoblanco, 28049 Madrid, and Centro Internacional de Física, Bogotá.

# 1 Introduction

A very concise summary of our main ideas and results on Standard Model (SM) baryogenesis in the presence of a first order phase transition, was recently presented in ref.[1]. An academic<sup>4</sup> scenario at zero temperature is developed with all the particulars in ref.[2]. The aim of the present work is to consider in detail the finite temperature ( $T$ ) scenario, where decoherence effects become essential.

Gamma-ray and cosmic data do not show any evidence for primary antiparticles on scales up to the level of clusters of galaxies. Nucleosynthesis constraints require a baryon number to entropy ratio in the observed part of the universe  $n_B/s \sim (4 - 6)10^{-11}$  at  $T > 1$  GeV [3]. In the absence of a sensible mechanism for matter-antimatter separation on such large scales, a plausible alternative is to require that the microscopic laws of physics are responsible for such a baryonic excess[4]. This scenario is called baryogenesis.

The SM electroweak phase transition occurs rather late in the cosmological evolution, at a time when the expansion of the universe is slow compared to weak interaction time scales and  $T \sim 100$  GeV. Sakharov's condition[4] of departure from thermal equilibrium could be fulfilled through a sudden, first order, phase transition[5][6]. In this case, bubbles of true ground state, characterised by a non-zero vacuum expectation value of the Higgs field  $v$ , grow and fill the preexisting  $v = 0$  universe. The evident non-equilibrium element is given by the propagation of the bubble surfaces, and physics in their vicinity should be examined in view of baryogenesis[7].

It has been known as well for many years that weak interactions violate baryon number[8]. At low temperatures, the rate is negligible, while at high temperatures[9] the rate is enhanced,

$$\Gamma_{sph}^u \sim \kappa(\alpha_W T)^4, \quad v = 0 \quad (1.1)$$

$$\Gamma_{sph}^b \sim \exp\left[-\frac{M_W(T)}{\alpha_W T}\right], \quad v \neq 0 \quad (1.2)$$

where  $v$  denotes the vacuum expectation value of the Higgs field, and  $\kappa$  is a parameter of  $O(1)$  or smaller.

The SM complies as well with the C and CP violation requirements. In particular the presence of complex Yukawa couplings induces a phase in the Cabibbo-Kobayashi-Maskawa (CKM)[10] matrix for three generations, responsible for CP violation.

Sakharov's conditions imply that both baryon number-violating and C and CP-violating processes have to undergo an out-of-equilibrium period. The currently proposed scenario for SM baryogenesis[11] is a charge transport mechanism [12]. It is graphically summarised in Fig. 1, where we have zoomed into the vicinity of one of the bubbles. In the wall rest frame a net baryonic flux is hitting the surface from the unbroken phase. Consider for definiteness the trajectory of an initial right-handed quark. Upon eventual reflection, a left-handed quark will travel backwards to the unbroken ( $v = 0$ ) phase. Electroweak interactions have been *a priori* active throughout the trajectory; their CP-violating effects induce a different reflection probability for quarks and antiquarks and, thus, a CP asymmetry in the reflected flux. Then,

---

<sup>4</sup>Academic because the physical first order phase transition is a thermal effect. In ref. [2] we considered an hypothetical  $T = 0$  world with two phases of spontaneous symmetry breaking separated by a thin wall, to sharpen our tools and disentangle the effects specific to the presence of a wall from the pure thermal ones.

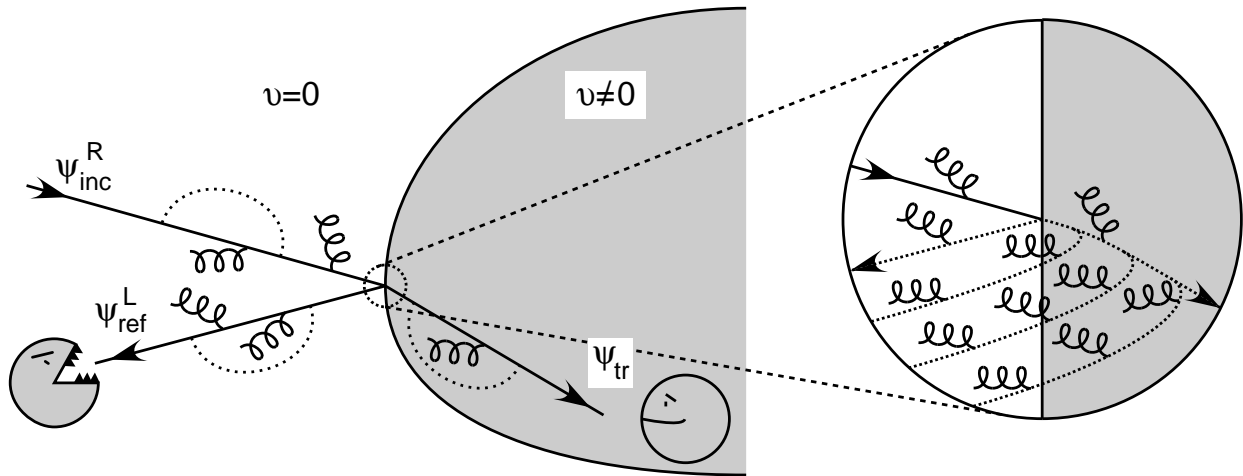


Figure 1: *Artistic view of the charge transport mechanism, as described in the text. The hungry “pacman” represents rapid sphalerons processes. The wiggly lines stand for collisions with thermal gluons. Only electroweak loops are depicted, represented by dotted lines.*

unsuppressed sphaleron processes, eq. (1.2), restoring equilibrium in the unbroken phase, can “swallow” the outgoing quarks, transforming the CP asymmetry into a baryonic one. The sweeping of the expanding bubble will automatically transfer the latter to the broken phase ( $v \neq 0$ ), where we live. An important survival requirement for the produced baryon asymmetry was given in refs. [13] and [14], by requiring that sphaleron processes inside the bubble are weak enough so as not to wash it out. In perturbation theory, this results in an upper bound of the Higgs mass  $\sim 45$  GeV, in conflict with experiment. This is a big problem for the scenario, although the perturbative treatment may be inadequate, and the question is the subject of much work at present.

We will not enter the discussion on whether a first order phase transition did take place. It will be assumed that it did, and that an optimal sphaleron rate is present as well. Our aim is to argue, on a quantitative estimation of the electroweak C and CP effects exclusively, that the current SM scenario is unable to explain the above mentioned baryon number to entropy ratio<sup>5</sup>. Notice that once a CP-asymmetry on the reflected baryonic current,  $\Delta_{CP}$ , is obtained, the induced baryon asymmetry is at most  $n_B/s \sim 10^{-2}\Delta_{CP}$ , in a very optimistic estimation of the non-CP ingredients[14][11].  $\Delta_{CP} \geq 10^{-8}$  is thus required.

The symmetries of the problem are analyzed in detail for a generic bubble in ref.[2]. Major unknowns of the scenario are the wall velocity,  $\vec{v}_{wall}$ , and the wall thickness,  $l$ . Typical values for  $|\vec{v}_{wall}|$  are non-relativistic,  $\sim 0.1-0.4$ [14][17]. Our analytical results correspond to the thin wall scenario. The latter provides an adequate physical description for typical momentum of the incoming particles  $|\vec{p}| \ll 1/l$ . For higher momenta the cutoff effects would show up, and indeed “realistic” walls have  $l \sim 10/T - 20/T$ , but it is reasonable to believe that the thin wall approximation produces an upper bound for the CP asymmetry. We work in a simplified scenario with just one spatial direction, perpendicular to the wall surface: phase

<sup>5</sup>A discussion of intuitive expectations is given in the introduction of ref.[2]

space effects in the 3 + 1 dimension case would further suppress the effect. It is assumed as well that both phases are in thermal equilibrium : this is only broken by the wall motion.

At  $T \neq 0$  the correct incoming asymptotic states are quasiparticles instead of particles, built up of a resummation of the thermal self-energies of the particles. Nevertheless, the three building blocks of the problem are essentially the same as in the  $T = 0$  case[2], to wit: the CP-violating couplings of the CKM matrix, the presence of CP-even phases associated to complex reflection coefficients for certain values of the energy of the incoming quasi-particles, and the well-known fact that, at  $T \neq 0$ , the fermionic on-shell self-energy cannot be completely renormalized away and induces physical transitions already at the one-loop level. Even starting from massless particles, the eigenstates of the effective thermal Dirac equation have an “effective mass”, or plasma frequency, due to the QCD thermal self-energies. It gives the overall energy scale of the problem  $\sim g_s T \sim 50$  GeV, for  $T \sim 100$  GeV. This results in a shift in the position of the reflection coefficient threshold for a given quasi-particle. Nevertheless, the tree-level reflection region for a given flavour is still of the order of the corresponding current (non-thermal) mass  $m$ . In other words, the time required for complete reflection of a given quasi-particle is of the order of  $1/m$ .

On top of the above, the authors of ref.[11] have pointed out that electroweak thermal loops are present as well, and because the latter are flavour dependent, their resummation can lift the QCD degeneracy of the spectrum of quasi-quarks even far from the wall in the unbroken phase<sup>6</sup>. The result would be further shiftings and reshufflings in the reflection coefficient thresholds<sup>7</sup> and, more important, a sizable CP asymmetry due to interference between different flavours and chiralities. In our opinion, the important point to retain is that CP violation is a quantum phenomenon, and can only be observed when quantum coherence is preserved over time scales larger than or equal to the electroweak time scales needed for CP violation.

We argue[1] that the quantum phase of the quasi-quarks is in fact lost much before the time scales mentioned in the above paragraphs. A further fundamental difference with the  $T = 0$  case is the damping rate,  $\gamma$ , of quasi-particles in a plasma. Small momenta are relevant for the problem under study, and it is known that at zero momentum, the QCD contribution to the damping rate is  $\gamma \sim 0.15 g_s^2 T$ , i.e.  $\sim 19$  GeV. Due to incoherent thermal scattering with the medium, the quasi-particle has a finite life-time  $\sim 1/2\gamma$ , turning eventually into a new state, out of phase with the initial one. Although the life-time is larger than the overall QCD time scale mentioned above,  $\sim 1/(50\text{GeV})$ , it is small in comparison with both the electroweak thermal self-energy time scales for any quasi-quark, and with the tree-level reflection times  $\sim 1/m$  for all quasi-quarks but the top.

The problem can be rephrased in terms of spatial decoherence. Reflection is a spatial property. The quasi-quarks have a group velocity of  $\sim 1/3$  and thus a mean free path, or coherence length, of  $\sim 1/6\gamma$ . Over larger scales, such as those needed for instance for total reflection, the quantum coherence of light quasi-quarks is damped and any pure quantum effect, such as CP violation, is suppressed.

We thus show that tree-level reflection is suppressed for any light flavour by a factor

---

<sup>6</sup>Unlike the  $T = 0$  case, Lorentz invariance is lost even far from (without) the wall. At  $T = 0$ , far from the wall in the unbroken phase, all particles are massless, at any order in the self-energy corrections. Any base is a good one, as rotations are physically irrelevant.

<sup>7</sup>We will see that, finally, it just amounts to technical complications.

$\sim m/2\gamma$ . The presently discussed CP-violation observable results from the convolution of this reflection effect with electroweak loops in which the three generations must interfere coherently in order to produce a CP-violation observable. It follows that further factors of this type appear in the final result, which is many orders of magnitude below what observation requires and has an “à la Jarlskog” [26] type of GIM cancellations. We show as well that the effect is present at order  $\alpha_W^2$  in a perturbative expansion, as in the  $T = 0$  case [2].

The scope of the present paper goes beyond the particular issue of baryon number generation in the SM. Spatial loss of quantum coherence may be relevant in other microscopic processes at finite temperature. A more rigorous treatment than the heuristic one developed here would be welcome, though. In our opinion, this general topic deserves further attention.

In Sect. 2 we discuss on general grounds the relation between baryonic and CP asymmetries. Sect. 3 describes the quasi-particle spectrum far from the wall both in the unbroken and the broken phase, as well as at the interface. It contains the dispersion relations, exemplified by the corresponding effective Lagrangians/Hamiltonians which take into account the QCD damping rate. Sect. 4 considers the tree-level scattering of a quasi-quark hitting the bubble wall from the unbroken phase in a one-flavour world. It parametrises how the loss of quantum coherence results in a damping of the reflection properties of the plasma. A density matrix formalism is developed as well. Sect. 5 considers the same scattering problem in the realistic case of three generations with mixing. It includes the computation of the CP asymmetry as well as comparison with literature and comments on wall thickness effects. The conclusions are summarised in Sect. 6.

## 2 Baryon Asymmetry Through Charge Transport

In the introduction, we have discussed qualitatively how it is possible to generate a baryon asymmetry in the context of a first order phase transition by fermion transport. In this section, we state more precisely the relation between the baryon asymmetry,  $n_b/s$ , and the CP-odd asymmetry that we aim to compute.

In the fermion transport mechanism, we can distinguish two steps. Firstly, a spatial chiral baryon number separation is produced due to the CP-violating scattering of quarks on the wall.

Denote by  $r_\chi^{u,b}$ ,  $t_\chi^{u,b}$  ( $\bar{r}_\chi^{u,b}$ ,  $\bar{t}_\chi^{u,b}$ ), the reflection and transmission amplitudes from the unbroken ( $u$ ) or broken ( $b$ ) phases, for an incoming quark (antiquark) of chirality  $\chi$ <sup>8</sup>. In our convention, a positive velocity is defined as flowing from the unbroken to the broken phase. The spin  $\sigma_z$  is a conserved quantum number. For positive (negative) group velocity, its eigenvalue in the unbroken phase is given by chirality  $+(-)\chi$ , as will be shown in section (3.2). In the broken phase, although chirality is no longer a good quantum number, we keep the same notation for the  $\sigma_z$  eigenvalues. The conserved current density in the  $z$ -direction is

$$j_z \propto \bar{u}(p')\gamma_z u(p) = V_z u^\dagger(p')u(p), \text{ for } p = p' \quad (2.1)$$

---

<sup>8</sup>For anti-quarks, the CP conjugate of a quark of chirality  $\chi$  has chirality  $-\chi$ . More precisely, the doublet quark (antiquark) has chirality  $-1 (+1)$ , and conversely for singlets. To simplify notations,  $\chi$  will indifferently stand for ( $L, R$ ) or the associated  $\gamma_5$  eigenvalue  $(-1, +1)$ .

where  $\vec{V}$  is the group velocity. For convenience we will extend eq. (2.1) to  $p \neq p'$ , in which case it may be taken as a definition of a “non diagonal”  $V_z$ . For an incoming spinor  $u_\chi^u$ , normalised as  $u_\chi^{u\dagger} u_\chi^u = 1$ , we have

$$\frac{j_{ref}}{j_{inc}} = |r_\chi^u|^2 |V_{-\chi}^u/V_\chi^u| = |r_\chi^u|^2, \quad \frac{j_{tr}}{j_{inc}} = |t_\chi^u|^2 |V_\chi^b/V_\chi^u|, \quad (2.2)$$

where we used  $|V_{-\chi}^u/V_\chi^u| = 1$ , consistent with our future approximations. The one particle thermal density matrix in the wall rest frame,  $\rho_\chi^{u,b}$ , is a positive definite hermitian matrix<sup>9</sup>. It is not translationally invariant (i.e. it is non-diagonal in momentum), due to the presence of the wall and depends on the plasma velocity,  $-v_{wall}$ . Also, it is different for doublet and singlet quarks, as electroweak interactions generate an  $O(\alpha_w)$  difference in their thermal self-energies.

The density matrix of incoming particles for one given chirality  $\chi$  is normalised as usual,

$$\int dp \text{Tr}[\rho_\chi^u(p, p)] = 1, \quad (2.3)$$

where Tr stands for the trace in flavour space. This corresponds to having one particle in the total volume  $L$ , i.e. to a particle density far from the wall of  $1/L$ .

The chiral baryon number current density in the unbroken phase, for a unit incoming density, is then given by the sum of the corresponding reflected and transmitted chiral current densities<sup>10</sup>,

$$\begin{aligned} \Delta_\chi^u \equiv & \frac{L}{2\pi} \int \int dp dp' \text{Tr}[\rho_{-\chi}^u(p, p') \{r_{-\chi}^u(p') r_{-\chi}^u(p)^\dagger - \bar{r}_\chi^u(p') \bar{r}_\chi^u(p)^\dagger\}] \\ & + |V_\chi^u|/\sqrt{|V_\chi^b(p) V_\chi^b(p')|} \text{Tr}[\rho_\chi^b(p, p') \{t_\chi^b(p') t_\chi^b(p)^\dagger - \bar{t}_{-\chi}^b(p') \bar{t}_{-\chi}^b(p)^\dagger\}]. \end{aligned} \quad (2.4)$$

This expression can be simplified by using the relations imposed by unitarity and CPT symmetry, or more exactly CP'T. The latter is defined [2] as the combination of CPT and a  $\pi$  rotation around the  $y$  axis, which leaves the wall invariant.

- CP'T

$$r_\chi^u = (\bar{r}_\chi^u)^t, \quad r_\chi^b = (\bar{r}_\chi^b)^t, \quad t_\chi^u = (\bar{t}_{-\chi}^u)^t \quad (2.5)$$

where superscript  $t$  stands for transposition in flavour space.

- Unitarity, i.e. current conservation,

$$r_\chi^u r_\chi^{u\dagger} + |V_\chi^b/V_\chi^u| t_\chi^u t_\chi^{u\dagger} = 1, \quad r_\chi^b r_\chi^{b\dagger} + |V_\chi^u/V_\chi^b| t_\chi^b t_\chi^{b\dagger} = 1. \quad (2.6)$$

---

<sup>9</sup>The density matrix for antiquarks of chirality  $-\chi$  is the same, if we assume there are no primeval asymmetries.

<sup>10</sup>In deriving 2.4 we have used the assumption (trivially verified for non-interacting particles prepared in equilibrium in a half space) that  $\rho_{-\chi}^u(p, p') r_{-\chi}^u(p') r_{-\chi}^u(p)^\dagger + \rho_\chi^b(p, p') t_\chi^b(p') t_\chi^b(p)^\dagger |V_\chi^u|/\sqrt{|V_\chi^b(p) V_\chi^b(p')|}$  is the matrix density for the particles of chirality  $\chi$  going away from the wall in the unbroken phase, and analogously for antiquarks. The full density matrix further has chirality non diagonal pieces, but these do not contribute to the computed current.

Then,

$$\Delta_\chi^u = \frac{L}{2\pi} \int \int dp dp' \text{Tr}[(\rho_{-\chi}^u - \rho_\chi^b)\{r_{-\chi}^u(r_{-\chi}^u)^\dagger - \bar{r}_\chi^u(\bar{r}_\chi^u)^\dagger\}] \quad (2.7)$$

where the possible flavour non-diagonal elements in  $(\rho_\chi^b)^t$  have been neglected, and the  $p, p'$  dependence omitted for simplicity.

The total outgoing baryon number current density in the unbroken phase, per unit incoming quark/antiquark flux, is:

$$B^u = \Delta_\chi^u + \Delta_{-\chi}^u = \frac{L}{2\pi} \int \int dp dp' \text{Tr}[(\rho_{-\chi}^u - \rho_\chi^u + \rho_{-\chi}^b - \rho_\chi^b)\{r_{-\chi}^u(r_{-\chi}^u)^\dagger - \bar{r}_\chi^u(\bar{r}_\chi^u)^\dagger\}] \quad (2.8)$$

For  $\rho_{-\chi}^{u,b} = \rho_\chi^{u,b}$ , clearly  $B^u = 0$ . This shows that, up to order  $O(\alpha_w)$ , only *chiral* baryon number gets separated by the wall. We will neglect this subleading effect and assume  $\rho_{-\chi}^{u,b} = \rho_\chi^{u,b} = \rho^{u,b}$  from now on.

Furthermore, neglecting the current (non-thermal) mass effects in the thermal distributions<sup>11</sup>,  $\rho^u$  and  $\rho^b$  only differ because of the opposite boost. If  $\rho^{u,b}$  were the boosted Fermi thermal distribution, and for small wall velocities,

$$\rho^u - \rho^b \simeq v_{wall} f \rho. \quad (2.9)$$

where  $\rho$  corresponds to the Fermi thermal distribution in the plasma rest frame,  $\rho \propto n_F$ , and  $f = \rho^{-1} \partial \rho / \partial v^{wall} < 1$ <sup>12</sup>. For the problem under study,  $\rho$  differs from the Fermi distribution, but the relation (2.9), with  $f < 1$ , should still be a good order of magnitude estimate.

In this approximation, we define the CP asymmetry as

$$\Delta_{CP} = \frac{L}{2\pi} \text{sign}(\chi) \int \int dp dp' \text{Tr}[\rho \{r_{-\chi}^u(r_{-\chi}^u)^\dagger - \bar{r}_\chi^u(\bar{r}_\chi^u)^\dagger\}]. \quad (2.10)$$

In a second step, the sphaleron transitions are taken into account. We do not consider strong sphalerons [15], which would further reduce the effect [16], as they require to take into account the  $O(\alpha_W)$  difference in the thermal distributions for doublets and singlets mentioned above. Weak sphalerons only affect left chirality particles (or right antiparticles). As explained in the introduction, these sphaleron processes have a very different rate in each phase, eqs. (1.1) and (1.2). In an ideal picture, all the left baryon number in the unbroken phase is completely diluted, while the one in broken phase remains. Eventually, when the phase transition is completed, the remaining total baryon number, divided by the original number  $n$  of quarks with one given chirality and spin, is

$$n_B^{optimal} / n = \frac{1}{3} \Delta_R^u = -\frac{1}{3} \Delta_L^u \simeq \frac{1}{3} v^{wall} \Delta_{CP}. \quad (2.11)$$

Only the contributions from the unbroken phase appear, as sphalerons transitions are absent from the broken phase.  $n_B^{optimal} / s$  is smaller, as the total entropy  $s$  is at least one order of magnitude larger than  $n$ <sup>13</sup>.

<sup>11</sup>This is a good approximation for quark masses smaller than  $g_s T$ .

<sup>12</sup>For the Fermi distribution,  $f = (1 - n_F) \frac{p^u - p^b}{T}$ , where  $p^u \simeq p, p'$  is the momentum in the unbroken phase, and  $p^b$  in the broken one.

<sup>13</sup>There are 4 spin-chiralities per quark and per antiquark, three generations, and additional quanta in the plasma (leptons and gauge bosons). Besides, the quasiparticles correspond to a limited part of phase space,  $E \sim g_s T$ .

Unfortunately, the sphaleron processes are not so efficient and computing the actual number of sphaleron transitions is a difficult diffusion problem. The authors of [11] give an already optimistic estimate for  $n_b/s$  which is  $\sim 10^{-2}\Delta_{CP}$ . Without relying on this calculation, it is necessarily true that

$$\frac{n_b}{s} < \Delta_{CP}. \quad (2.12)$$

$\Delta_{CP}$  gives a highly conservative upper bound for  $n_b/s$ . This will be enough to rule out SM baryogenesis within this mechanism, and we will devote the rest of the paper to the computation of this asymmetry.

### 3 The spectrum of quasi-particles.

In this section the spectrum of quasiparticles is derived from the thermal loop contribution to the quark self-energy. The solutions in a world with just one phase, either spontaneously broken ( $v \neq 0$ ) or unbroken ( $v = 0$ ), are computed first. Secondly, the case when the two phases coexist separated by a boundary (thin wall) is discussed, as well as the matching of the two spectra.

#### 3.1 The quark self-energy.

This is a rather technical subsection, whose results are needed later. We present a novel calculation of the real part of the self-energy, including the electroweak contributions, in the broken phase. The computations are performed in the real time formalism. We compare to previous results for the unbroken phase. The imaginary part computed in QCD at zero momentum[19] is considered.

##### 3.1.1 Real part in the broken phase.

We use the notations of [22], generalised to several flavours:

$$\text{Re}(\Sigma(k)) = -a\cancel{k} - b\not{u} - cm \quad (3.1)$$

where  $a$ ,  $b$ ,  $c$  and  $m$  are Lorentz invariant matrices in flavour space,  $u$  is the four-velocity of the plasma and  $k = (\omega, \vec{k})$  is the external momentum.  $m$  denotes the mass matrix for the external flavours. In the plasma rest frame and the mass basis,

$$\text{Re}(\Sigma(\omega, \vec{k}))\gamma_0 = -h(\omega, \vec{k}) - a(\omega, \vec{k})\vec{\alpha} \cdot \vec{k} - c(\omega, \vec{k})m\gamma_0 \quad (3.2)$$

where

$$h(\omega, \vec{k}) = a(\omega, \vec{k})\omega + b(\omega, \vec{k}). \quad (3.3)$$

The one loop calculation gives the following matrix elements:

$$a(\omega, k)_{fi} = f A(m_i, 0)\delta_{fi} + \frac{g^2}{2} \left[ \sum_l f_{W,l} A(M_l, M_W) + (f_Z A(m_i, M_Z) + f_H A(m_i, M_H))\delta_{fi} \right] \quad (3.4)$$



where the index  $l$  runs over the internal flavours for  $W$  exchange, and  $M$  denotes the corresponding mass. In this expression,

$$f = \left[\frac{4}{3}g_s^2 + Q_i^2 g^2 s_W^2\right](L + R) \quad , \quad f_{W,l} = \left[\left(1 + \frac{\lambda_i^2}{2}\right)L + \frac{\lambda_i \lambda_f}{2}R\right]K_{li}K_{lf}^* \\ f_Z = \frac{1}{2}\left(\frac{4}{c_W^2}(T_i^3 - Q_i s_W^2)^2 + \frac{\lambda_i^2}{2}\right)L + \left(\frac{4}{c_W^2}(-Q_i s_W^2)^2 + \frac{\lambda_i^2}{2}\right)R \quad , \quad f_H = \frac{\lambda_i^2}{4}(L + R), \quad (3.5)$$

where  $L, R$  are chiral projectors.  $K$  represents the Cabibbo-Kobayashi-Maskawa matrix and  $\lambda_i = m_i/M_W$  are related to the usual Yukawa couplings by the following relation,

$$f_i = \frac{g\lambda_i}{\sqrt{2}}. \quad (3.6)$$

The integral is given by:

$$A(M_F, M_B) = \frac{1}{k^2} \int_0^\infty \frac{dp}{8\pi^2} \left( \left[ -\frac{(\omega^2 + k^2 + \Delta)}{2k} \frac{p}{E_B} L_I^+(p) - \frac{\omega p}{k} L_I^-(p) + \frac{4p^2}{E_B} \right] n_B(E_B) + \right. \\ \left. \left[ \frac{\omega^2 - k^2 - \Delta}{2k} \frac{p}{E_F} L_{II}^+(p) - \frac{\omega p}{k} L_{II}^-(p) + \frac{4p^2}{E_F} \right] n_F(E_F) \right), \quad (3.7)$$

where

$$L_I^\pm(p) = \left[ \log \frac{2kp + 2E_B\omega + \omega^2 - k^2 + \Delta}{-2kp + 2E_B\omega + \omega^2 - k^2 + \Delta} \right] \pm [E_B \rightarrow -E_B] \quad (3.8)$$

and

$$L_{II}^\pm(p) = -\left[ \log \frac{2kp - 2E_F\omega + \omega^2 - k^2 - \Delta}{-2kp - 2E_F\omega + \omega^2 - k^2 - \Delta} \right] \mp [E_F \rightarrow -E_F], \quad (3.9)$$

with

$$E_{F,B} = \sqrt{p^2 + M_{F,B}^2}, \quad \Delta = M_B^2 - M_F^2, \quad n_{F,B}(E) = (\exp E/T \pm 1)^{-1}. \quad (3.10)$$

The function  $h(\omega, k)$  is given by

$$h(\omega, k)_{fi} = -f H(m_i, 0)\delta_{fi} - \frac{g^2}{2} \left[ \sum_l f_{W,l} H(M_l, M_W) + (f_Z H(m_i, M_Z) + f_H H(m_i, M_H))\delta_{fi} \right], \quad (3.11)$$

where

$$H(M_F, M_B) = \frac{1}{k} \int_0^\infty \frac{dp}{8\pi^2} \left( [pL_I^-(p) + \frac{\omega p}{E_B} L_I^+(p)] n_B(E_B) + pL_{II}^-(p) n_F(E_F) \right). \quad (3.12)$$

The chirality breaking term  $c(\omega, k)$  has the following expression

$$c(\omega, k)_{fi} = 2f C(m_i, 0)\delta_{fi} + \frac{g^2}{2} \left[ \sum_l \frac{M_l}{m_i} g_{W,l} C(M_l, M_W) + \right. \\ \left. (g_Z C(m_i, M_Z) - f_H C(m_i, M_H))\delta_{fi} \right], \quad (3.13)$$

with

$$g_{W,l} = \frac{\lambda_M}{2}(\lambda_f L + \lambda_i R) K_{li} K_{lf}^*, \quad g_Z = \frac{1}{2}[-8Q_i \frac{s_W^2}{c_W^2}(T_3 - Q_i s_W^2) + \frac{\lambda_i^2}{2}](L + R) \quad (3.14)$$

and

$$C(M_F, M_B) = \frac{1}{k} \int_0^\infty \frac{dp}{8\pi^2} \left( \frac{p}{E_B} L_I^+(p) n_B(E_B) + \frac{p}{E_F} L_I^+(p) n_F(E_F) \right). \quad (3.15)$$

### 3.1.2 Real part in the unbroken phase.

In the unbroken world the expressions (3.4)-(3.15) apply with all masses equal to zero. For the sake of comparison with previous literature, we give here the leading ( $O(T^2)$ ) contribution when  $\omega, |\vec{k}| \ll T$ . In this limit, the one loop fermionic self energy in the unbroken phase has been computed in QCD [20], [21] and generalised to electroweak interactions in [11]. We find:

$$h(\omega, \vec{k})_L = -\frac{T^2}{\omega} F\left(\frac{\omega}{|k|}\right) \left\{ \frac{2\pi\alpha_s}{3} + \frac{3\pi\alpha_W}{8} \left( 1 + \frac{\tan^2 \theta_W}{27} + \frac{1}{3}(\lambda_i^2 + K_{lf}^* \lambda_l^2 K_{li}) \right) \right\}, \quad (3.16)$$

$$h(\omega, \vec{k})_R = -\frac{T^2}{\omega} F\left(\frac{\omega}{|k|}\right) \left\{ \frac{2\pi\alpha_s}{3} + \frac{\pi\alpha_W}{2} \left( Q_i^2 \tan^2 \theta_W + \frac{1}{2} \lambda_i^2 \right) \right\}, \quad (3.17)$$

with

$$a(\omega, \vec{k})_L = -h(\omega, \vec{k})_L \frac{\omega \left( 1 - F\left(\frac{\omega}{|k|}\right) \right)}{|k|^2 F\left(\frac{\omega}{|k|}\right)}, \quad (3.18)$$

and

$$a(\omega, \vec{k})_R = -h(\omega, \vec{k})_R \frac{\omega \left( 1 - F\left(\frac{\omega}{|k|}\right) \right)}{|k|^2 F\left(\frac{\omega}{|k|}\right)}. \quad (3.19)$$

$a_{L,R}, h_{L,R}$  correspond to the coefficients of the projectors  $L, R$  in  $a, h$ , and

$$F(x) = \frac{x}{2} \left( \log \left( \frac{x+1}{x-1} \right) \right). \quad (3.20)$$

In eqs. (3.16)-(3.19) it is understood that all terms which do not contain the CKM matrix are flavour diagonal<sup>14</sup>.

### 3.1.3 Imaginary part of the Self-energy.

It is known that the one loop calculation of the imaginary part of the self energy (proportional to the damping rate) is incomplete. A leading order QCD computation of the quasi-quark damping rate[19] has been performed at zero  $\vec{k}$ :  $\gamma \sim 0.15g_s^2 T$  i.e.  $\sim 19$  GeV at  $T = 100$  GeV. We will neglect its electroweak component, and assume that in the vicinity of  $\vec{k} = 0$  the damping rate remains close to the above-mentioned value, i.e.

$$\gamma_0 \text{Im}(\Sigma(\omega, \vec{k})) \simeq -2\gamma \quad (3.21)$$

---

<sup>14</sup>The careful reader may notice several differences in numerical factors between eqs (3.16)-(3.19) and eqs. (6.6)-(6.8) in [11], once the change of basis is taken into account.

### 3.2 The spectrum.

The spectrum of quasi-particles in a quark-gluon plasma with only QCD interactions has been extensively studied in the literature [20], [21]. The effects we need for generating a baryon asymmetry are electroweak, though, and it is necessary to include the electroweak thermal loops. The latter will modify the spectrum in a complicated way, although the corrections are quantitatively small with respect to the QCD contributions. This will allow a convenient perturbative treatment, as it will be shown.

Let us summarise first the results in pure QCD, i.e. setting  $\alpha_w = 0$  in the self-energies (3.2). The spectrum of quasi-particles is given by the isolated poles of the propagator (or the zeros of the self-energy). At  $\vec{k} = 0$ , it is given by the solution of

$$\omega + h_{QCD}(\omega, 0) - 2i\gamma = 0 \quad (3.22)$$

To gain some insight into the energy scale of the spectrum, we simplify (3.22) neglecting all the energy scales other than  $T$  (i.e.  $m_i \ll T$ ). We work to first order in  $\gamma/(g_s T)$ , an approximation we will stick to in the rest of the paper. The solution then is

$$w_{QCD}^0 \simeq T \sqrt{\frac{2\pi\alpha_s}{3}} - i\gamma \equiv \omega_{QCD}^0 - i\gamma. \quad (3.23)$$

Eq. (3.23) shows that QCD has shifted dramatically the position of the singularities of the quark propagator (by singularity we mean the pole and the location of the thermal  $\delta(p^2 - m^2)$ 's), and sets the energy scale of the quasi-particles at  $O(g_s T) \sim 50$  GeV.

The dispersion relations  $w(\vec{k})_{QCD}$  satisfied by these quasi-particles are given by the vanishing eigenvalues of the matrix

$$i\gamma_0 S^{-1} = \omega + h_{QCD}(\omega, \vec{k}) - \gamma_5(\vec{\sigma} \cdot \vec{k})(1 + a_{QCD}(\omega, \vec{k})) - 2i\gamma. \quad (3.24)$$

We are interested only in the low momentum region, and upon linearising in momentum we find,

$$w(\vec{k})_{QCD} = \omega_{QCD}^0 + \chi(\vec{\sigma} \cdot \vec{k})V_{QCD} - i\Gamma_{QCD}, \quad (3.25)$$

where  $\chi$  is the eigenvalue of  $\gamma_5$  (the chirality), i.e.  $+1(-1)$  for right(left)-handed fermions, and

$$V_{QCD} \equiv \frac{1 + a_{QCD}(\omega_{QCD}^0, 0)}{s_{QCD}(\omega_{QCD}^0, 0)}, \quad \Gamma_{QCD} = \frac{2\gamma}{s_{QCD}(\omega_{QCD}^0, 0)}, \quad (3.26)$$

with

$$s_{QCD}(\omega_{QCD}^0, 0) = 1 + \frac{\partial h_{QCD}(\omega, 0)}{\partial \omega} \Big|_{\omega_{QCD}^0}. \quad (3.27)$$

The functions  $s_{QCD}$  are the inverse of the residues at the poles. In a second quantisation treatment of the quasi-particles, they can be absorbed through wave function renormalisation, in order to properly normalise the kinetic terms. When deriving eq. (3.25) higher orders in  $\gamma/(g_s T)$  have been consistently neglected, leading to real arguments in eqs. (3.26) and (3.27).

The spectrum is obviously flavour and chiral degenerate, and that equation (3.25) holds separately for each flavour. For simplicity let us take  $\vec{k}$  along the  $z$  axis.  $V_{QCD}$  has a simple

meaning: up to a sign it is equal to  $\partial\omega(\vec{k})_{QCD}/\partial k_z$ , the group velocity of the wave packet. From eqs. (3.16)-(3.19) it is easy to see that, at leading  $T^2$  order,  $s_{QCD} = 2$  and the group velocity is  $\pm 1/3$ . More precisely, for a given value of  $k_z$  and a given flavour, there are four solutions: two possible chiralities and two possible helicities. The group velocity is given by the eigenvalue of  $\sim 1/3\gamma_5\sigma_z = 1/3\gamma_5\sigma_z(\hat{k}_z)^2$  i.e.  $1/3\chi h\hat{k}_z$ , where  $h$  is twice the helicity,  $\chi$  the chirality and  $\hat{k}_z = k_z/|k_z|$ . As a result, the group velocity has the same sign as the momentum when the chirality equals helicity. The solutions with opposite chirality and helicity are disregarded at zero  $T$  since they correspond to negative energy states. At finite  $T$ , due to the shift of the energy, part of these branches become physical. They are often called ‘‘abnormal’’ branches. As a consequence, for a given value of  $k_z$ , a normal and an abnormal branch have opposite slopes and there is generally one level crossing in the spectrum. It is also obvious from the above that positive (negative) group velocity corresponds to  $\gamma_5 = \sigma_z$  ( $\gamma_5 = -\sigma_z$ ). The two normal (abnormal) branches are degenerate.

For large  $|\vec{k}|$  the dispersion relations become non linear and the residues of the abnormal branches are exponentially small  $\sim \exp(-|\vec{k}|^2/\omega_{QCD}^2)$ ,  $|\vec{k}| \gg \omega_{QCD}$ , implying that abnormal excitations become irrelevant at large momentum<sup>15</sup>. However, we will restrict to the region where the linear approximation is appropriate, i.e. for momentum  $|\vec{k}| \ll \omega_{QCD}^0$ .

In what follows, we consider the electroweak contributions that lift the chiral and flavour degeneracy of the spectrum, together with subleading effects. We discuss separately the asymptotic spectrum in the unbroken and broken phases, which differ in the quark mass effects. In the real situation, with both phases separated by a thin wall interface, it is necessary to connect both asymptotic spectra and further approximations will be performed. In the following subsections, we start by considering the toy example of one generation in order to disentangle the mixing effects and, finally, we formulate the problem for several generations. Weak effects are not taken into account in the damping rate, which will then be the same for both chiralities and every flavour:

$$\Gamma_L = \Gamma_R = \Gamma_{QCD}. \quad (3.28)$$

### 3.2.1 Asymptotic Spectrum for one generation.

#### • Unbroken Phase

The procedure is the same as in the case of QCD, although taking the functions  $h(\omega, \vec{k})$  and  $a(\omega, \vec{k})$  as given by eqs. (3.11), (3.4) with vanishing masses and  $\alpha_w \neq 0$ , for one generation. They will be different for right and left chiralities: the degeneracy of the normal (abnormal) branches is lifted. We start with the one-loop self-energies in the mass basis,

$$i\gamma_0(S^{-1})^u = \begin{pmatrix} \omega + h_R^u - \vec{\sigma} \cdot \vec{k}(1 + a_R^u) - 2i\gamma & 0 \\ 0 & \omega + h_L^u + \vec{\sigma} \cdot \vec{k}(1 + a_L^u) - 2i\gamma \end{pmatrix}, \quad (3.29)$$

---

<sup>15</sup>This, as well as the doubling of the number of poles corresponding to particles carrying a given charge, is quite natural when recalling that annihilation operators can act non-trivially on a thermal state, to create a physical ‘‘hole’’. Clearly, for momenta so large that the corresponding state is not thermally occupied, we expect a strong suppression.

where the index  $u$  refers to the unbroken phase, and the functional dependence of  $h$ 's and  $a$ 's is kept implicit. The on-shell states correspond to the zeros of the determinant of  $i\gamma_0(S^{-1})^u$ , and the corresponding eigenstates verify the effective Dirac equation

$$i\gamma_0(S^{-1})^u\psi = 0. \quad (3.30)$$

At  $\vec{k} = 0$ , the solutions are given by the equation

$$w_{L,R}^u + h_{L,R}^u(w_{L,R}^u, 0) - 2i\gamma = 0. \quad (3.31)$$

As we are interested in the low momentum quasi-particles, we expand the effective Dirac operator around these poles and linearise in momentum. We also neglect  $O(\gamma/g_s T)$ ,

$$i\gamma_0(S^{-1})^u \frac{1 \mp \gamma_5}{2} = [1 + \frac{\partial h}{\partial \omega}|_{\omega_{L,R}^u}](\omega - w_{L,R}^u) - \gamma_5(1 + a_{L,R}^u)\vec{\sigma} \cdot \vec{k}, \quad (3.32)$$

where we have used the momentum independence of  $\gamma$ .

The solution for the dispersion relation at small momentum is then,

$$w(\vec{k})_{L,R} = \omega_{L,R}^u + \chi(\vec{\sigma} \cdot \vec{k})V_{L,R}^u - i\Gamma_{L,R}^u \quad (3.33)$$

where, as before,  $\omega_{L,R}^u = \text{Re}(w_{L,R}^u)$  and

$$V_{L,R}^u = \frac{1 + a_{L,R}^u(\omega_{L,R}^u, 0)}{s_{L,R}^u(\omega_{L,R}^u, 0)}, \quad \Gamma_{L,R}^u = \frac{2\gamma}{s_{L,R}^u(\omega_{L,R}^u, 0)}, \quad (3.34)$$

with

$$s_{L,R}^u(\omega_{L,R}^u, 0) = 1 + \frac{\partial h_{L,R}^u(\omega, 0)}{\partial \omega}|_{\omega_{L,R}^u}. \quad (3.35)$$

The spectrum (3.33) is illustrated in fig. 2(a). Even without quark masses, the degeneracy between L, R is now broken by the weak interactions due to thermal effects.

In the regime of low momentum (3.33), the dispersion relation is well described by the following effective Lagrangian for free quasi-particles:

$$\begin{aligned} \mathcal{L}_{eff} = & \Psi_L^\dagger (i\partial_t - iV_L^u \vec{\partial} \cdot \vec{\sigma} - \omega_L^u) \Psi_L + \Psi_R^\dagger (i\partial_t + V_R^u i\vec{\partial} \cdot \vec{\sigma} - \omega_R^u) \Psi_R \\ & + i\Psi_L^\dagger \Gamma_L^u \Psi_L + i\Psi_R^\dagger \Gamma_R^u \Psi_R, \end{aligned} \quad (3.36)$$

where  $\Psi_L$  and  $\Psi_R$  are respectively the left-handed and right-handed fields that create quasi-particles with the given chirality.  $\mathcal{L}_{eff}$  is not hermitian due to the damping rate.

### • Broken Phase

In this case, the self-energy is given by

$$i\gamma_0(S^{-1})^b = \begin{pmatrix} \omega + h_R^b - \vec{\sigma} \cdot \vec{k}(1 + a_R^b) - 2i\gamma & (1 - c)m \\ m^\dagger(1 - c)^\dagger & \omega + h_L^b + \vec{\sigma} \cdot \vec{k}(1 + a_L^b) - 2i\gamma \end{pmatrix}. \quad (3.37)$$

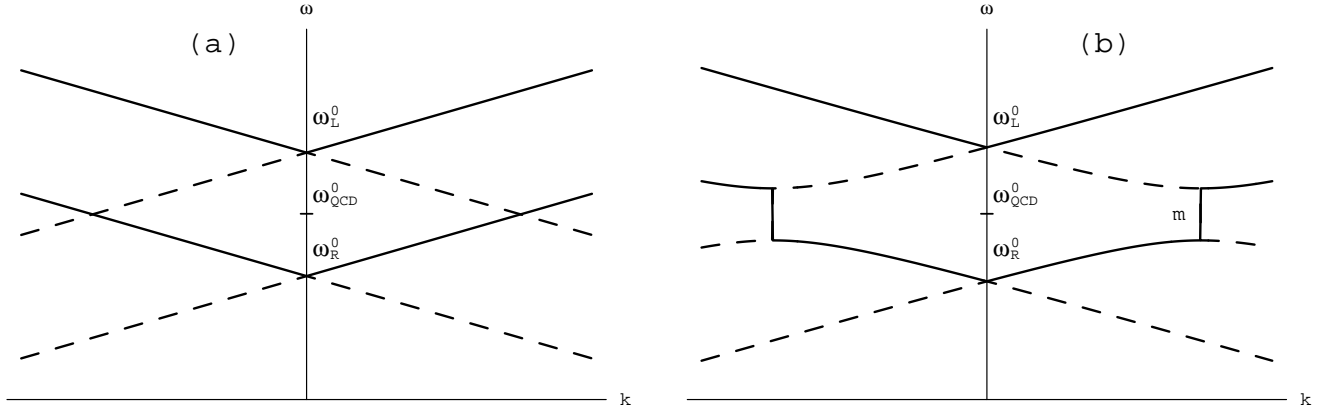


Figure 2: *Dispersion relations for quasi-particles in the (a) unbroken and (b) broken phases. The full (dashed) lines are normal (abnormal) branches. The upper (lower) lines correspond to left (right) chirality. When only QCD loops are considered, upper and lower branches are degenerate and intersect the vertical axis at  $\omega_{\text{QCD}}^0$ . The vertical lines in (b) represent the gaps of width  $\simeq m$ , in which total reflection occurs.*

The dispersion relations  $w(\vec{k})$  defining quasi-particles are given by the zeros of the determinant of (3.37). In the real part, the effect of the mass is to replace the two lines of the unbroken spectrum by a hyperbola. This is again quite similar to the  $T = 0$  scenario, except that the center of the hyperbolas is not necessarily at the origin. Between the minimum and maximum of the hyperbolas branches, an energy gap of width  $\sim m$  appears around the center. In this energy gap no plasma excitation can exist. This new spectrum is illustrated in fig. 2 (b).

These very narrow energy gaps are physically crucial since they induce total reflection of a quasiparticle coming from the unbroken phase with its energy precisely ranging in this gap. However, as we shall argue later, the large value of the damping rate prevents the existence of quasiparticles with such a small energy band.

In order to find the asymptotes we first consider the case  $\vec{k} = 0$  with vanishing non-diagonal terms in eq. (3.37). The centers of the hyperbolas are given by

$$\omega_{L,R}^b + h_{L,R}^b(\omega_{L,R}^b, 0) = 0 \quad (3.38)$$

They are slightly different to those in the unbroken phase, real part of eq. (3.31), due to mass effects in  $h^b$ . The solution with  $m = 0$ ,  $|\vec{k}|$  small, is similar to the one in the preceding subsection (3.33), with different values of  $V_{L,R}$  and  $s_{L,R}$ . A numerical estimate for down quarks gives a group velocity  $V_L^b = V_R^b = 0.339$  and  $s_{L,R}^b(\omega_{L,R}^b, 0) = 1.89$ , close to the values  $1/3$  and  $2$ , respectively, obtained with the unbroken loop at order  $T^2$ . For  $u$  and  $c$  quarks we obtain  $V_L^b = V_R^b = 0.346$  and  $h_{L,R}^b(\omega_{L,R}^b, 0) = 1.88$ , while for the top the results are  $0.165$  and  $2.5$ , respectively.

In the same way as we did for the unbroken phase, it is possible to obtain the effective Lagrangian for quasi-particles in the broken phase for the low momentum regime,

$$\begin{aligned} \mathcal{L}_{eff} = & \Psi_L^\dagger (i\partial_t - iV_L^b \vec{\partial} \cdot \vec{\sigma} - \omega_L^b) \Psi_L + \Psi_R^\dagger (i\partial_t + V_R^b i\vec{\partial} \cdot \vec{\sigma} - \omega_R^b) \Psi_R \\ & + i\Psi_L^\dagger \Gamma_L \Psi_L + i\Psi_R^\dagger \Gamma_R \Psi_R - (\Psi_L^\dagger \mu \Psi_R + \Psi_R^\dagger \mu^\dagger \Psi_L) \end{aligned} \quad (3.39)$$

where  $V_{L,R}^b, \Gamma_{L,R}^b$  are defined in terms of  $h^b, a^b$  analogously to eqs. (3.34) and (3.35), and

$$\mu = \frac{m(1 - c^b(\omega_R^b, 0))}{s_L^{b\,1/2}(\omega_L^b, 0) s_R^{b\,1/2}(\omega_R^b, 0)}. \quad (3.40)$$

### • The Interface Unbroken-Broken

The real problem we want to solve is the scattering of quasi-particles on the interface between the broken and unbroken phases. The usual procedure in scattering theory involves matching the in-states (asymptotic states in the unbroken phase) to the out-states (asymptotic states in the broken phase) through a unitary scattering matrix. The problem is, however, that the spectrum of single quasi-particle states do not form a complete basis, or in other words, the residues of all the single quasi-particle states do not sum up to one<sup>16</sup>his is usually associated with collisionless damping which is neglected here altogether. In massless QCD (as in NR plasmas), this type of Landau damping only becomes relevant for large enough momenta and we expect the same to be true here. . In fact, we have seen that these residues  $s_{L,R}^{u,b}$  are different for L or R quasi-particles and depending on whether they are in the broken or unbroken phase. This is a small correction coming from the subleading effects in T, so in order to simplify the problem we will neglect them when obtaining the asymptotic spectrum. Thus, we will only include in the determination of the quasi-particle dispersion relations the following corrections:

- QCD corrections at leading T.
- Diagonal Weak Interactions corrections leading in T.
- Linear terms in momentum.

This approximation ensures that the residues of the dispersion relations (or wave function renormalisation constants) are the same at both sides of the wall and equal for both chiralities.

In this approximation, the poles in the unbroken phase are given by the equation

$$w_{L,R}^0 + \bar{h}_{L,R}(w_{L,R}^0, 0) - 2i\gamma = 0, \quad (3.41)$$

where  $\bar{h}_{L,R}(\omega, k)$  contains only the leading-T QCD and diagonal weak corrections of (3.11). Now, expanding  $i\gamma_0(S_0^{-1})^u$  around these poles and linearising in momentum,

$$i\gamma_0(S_0^{-1})^u \frac{1 \mp \gamma_5}{2} = [1 + \frac{\partial \bar{h}}{\partial \omega}|_{\omega_{L,R}^0}](\omega - w_{L,R}^0) - \gamma_5(1 + \bar{a}_{L,R}^u) \vec{\sigma} \cdot \vec{k}, \quad (3.42)$$

---

<sup>16</sup>T

with  $\bar{a}_{L,R}(\omega, k)$  containing the leading-T, QCD and diagonal weak corrections in the functions (3.4). Using eqs.(3.16)-(3.19), together with the expansion  $F(x) \sim 1 + \frac{1}{3x^2}$ ,  $x \gg 1$  we get, to leading order in  $\gamma/(g_s T)$ ,

$$1 + \bar{a}_{L,R}(\omega^0_{L,R}, 0) = \frac{2}{3}, \quad (3.43)$$

$$1 + \frac{\partial \bar{h}_{L,R}}{\partial \omega} \Big|_{\omega^0_{L,R}} = 2, \quad (3.44)$$

Notice that although  $\bar{h}_{L,R}$  is flavour dependent, the pole condition in eq. (3.41) implies that the above results, eqs. (3.43) and (3.44) are not. The damping rate is

$$\Gamma = \frac{2\gamma}{1 + \frac{\partial \bar{h}_{L,R}}{\partial \omega} \Big|_{\omega^0_{L,R}}} = \gamma. \quad (3.45)$$

The dispersion relations describing the quasi-particles in the unbroken phase are given by the zeros of eq. (3.42):

$$w(k)_{L,R} = \omega^0_{L,R} + \chi \frac{1}{3} \vec{\sigma} \cdot \vec{k} - i\gamma. \quad (3.46)$$

In the broken phase, the only difference with respect to eq.(3.46), in this approximation, results from the  $L, R$  mixing effects due to the tree level mass. Thus, using eq. (3.42),

$$i\gamma_0(S_0^{-1})^b = i\gamma_0(S_0^{-1})^u + \begin{pmatrix} 0 & \frac{m}{2} \\ \frac{m^\dagger}{2} & 0 \end{pmatrix}, \quad (3.47)$$

where we have neglected the functions  $c(\omega, k)$  because they are subleading in T. The dispersion relations in the broken phase are just given by the determinant of  $i\gamma_0(S_0^{-1})^b$ .

From (3.42) and (3.47), we can easily write the effective unperturbed Hamiltonian for quasi-particles in the presence of a wall, in the basis of asymptotic states in the unbroken phase,

$$H_{eff}^0 = \begin{pmatrix} -\frac{1}{3}i\sigma_z\partial_z - i\gamma + \omega_R^0 & \frac{m}{2}\theta(z) \\ \frac{m}{2}\theta(z) & \frac{1}{3}i\sigma_z\partial_z - i\gamma + \omega_L^0 \end{pmatrix}. \quad (3.48)$$

### 3.2.2 Several generations.

In the case of several generations, the exact solution of the spectrum is very complicated, as the functions (3.4), (3.11), (3.13) are non-diagonal  $3 \times 3$  matrices in flavour space. In particular,  $h(\omega, k)$  and  $1 + a(\omega, k)$  may not be diagonalisable in the same basis, in such a way that single quasi-particle asymptotic states cannot be chosen to be diagonal in flavour. In order to simplify the problem, we will derive the dispersion relations for asymptotic quasi-particle states neglecting flavour mixing and, as we did for the one-flavour case, neglecting also the subleading effects in T, both in QCD and weak corrections. As previously stated,



in this way the residues of the dispersion relations are the same at both sides of the wall, for any flavour and chirality.

We start with the  $6 \times 6$  one-loop effective Dirac operator in the mass basis:

$$i\gamma_0(S^{-1})^u = \begin{pmatrix} \omega + h_R^u - \vec{\sigma} \cdot \vec{k}(1 + a_R^u) - 2i\gamma & 0 \\ 0 & \omega + h_L^u + \vec{\sigma} \cdot \vec{k}(1 + a_L^u) - 2i\gamma \end{pmatrix}, \quad (3.49)$$

$$i\gamma_0(S_0^{-1})^b = \begin{pmatrix} \omega + h_R^b - \vec{\sigma} \cdot \vec{k}(1 + a_R^b) - 2i\gamma & (1 - c)m \\ m^\dagger(1 - c)^\dagger & \omega + h_L^b + \vec{\sigma} \cdot \vec{k}(1 + a_L^b) - 2i\gamma \end{pmatrix}. \quad (3.50)$$

The results of the previous section hold here, if we substitute all  $\omega_{L,R}^0$  and  $h$ ,  $a$  and  $c$  by  $3 \times 3$  matrices. The expressions for  $h^b$ ,  $a^b$  and  $c^b$  ( $h^u$ ,  $a^u$  and  $c^u$ ) were given in subsection (3.1.2) with masses different from (equal to) zero. The effective unperturbed Hamiltonian for free quasi-particles is then

$$H_{eff}^0 = \begin{pmatrix} -\frac{1}{3}i\sigma_z\partial_z - i\gamma + \hat{\omega}_R^0 & \frac{m}{2}\theta(z) \\ \frac{m}{2}\theta(z) & \frac{1}{3}i\sigma_z\partial_z - i\gamma + \hat{\omega}_L^0 \end{pmatrix}, \quad (3.51)$$

where  $\hat{\omega}_R^0$  and  $\hat{\omega}_L^0$  are  $3 \times 3$  diagonal matrices  $(\omega_R^{01}, \omega_R^{02}, \omega_R^{03})$ ,  $(\omega_L^{01}, \omega_L^{02}, \omega_L^{03})$ , respectively.

In section (5), we will see that it is possible and consistent to include the remaining effects (non-leading and mixing) as a perturbation, without modifying the asymptotic states.

### 3.3 The damping rate.

Due to incoherent thermal scattering with the medium, the energy and momentum of the quasi-quarks in a plasma are not sharply defined, but spread like a resonance of width  $\gamma$  [19].

The QCD damping rate at zero momentum is of the order  $\gamma \sim 0.15 g_s^2 T$  [19], i.e.  $\sim 19$  GeV at  $T = 100$  GeV. Compared to the energy of the quasiparticle, of  $O(g_s T)$ , the damping rate is formally small, i.e. it contains one additional power of  $g_s$ . This hierarchy allows to speak of the mere existence of quasiparticles as coherent excitations<sup>17</sup>.

The quasi-particle has thus a finite life-time  $\sim 1/2\gamma$ , turning eventually into a new state, out of phase with the initial one. As the group velocity is of order  $1/3$ , the mean free path is of order  $1/6\gamma \sim 1/120$  GeV<sup>-1</sup>. Even if it is true that the relative phase between different quark flavours is not destroyed by collisions with the QCD thermal bath, it should be stressed that the quantum spatial coherence, i.e. the phase relation between points separated by a distance  $\geq 1/6\gamma$ , is lost.

The imaginary part of the QCD self-energy is much larger than the real part of the electroweak self-energy. For all quarks but the top, it is also much larger than the corresponding mass gap in the broken phase discussed in subsection (3.2.1). In other words, as we shall see explicitly later, the coherent electroweak processes relevant in the following require a time much larger than the mean free time of the quasiparticles.

---

<sup>17</sup>In practice however  $g_s$  is not so small, and the width of  $\sim 20$  GeV is not really small compared to the energy  $\sim 50$  GeV. We could say that quasi particles hardly exist. The plasma is mainly an incoherent mixture of states.

## 4 Reflection on the bubble wall: one flavour case.

In this section we discuss a world with just one flavour, and the tree-level reflection properties when a quasi-particle hits the boundary (thin wall approximation) separating the two phases of spontaneous symmetry breaking. No electroweak effect is considered, other than the mass of the quasi-particle. We quantitatively derive the dramatic effect of the QCD damping rate on the reflected density of quasi-quarks. After some considerations in terms of damped waves, the system is described in terms of wave-packets which exemplify the mean free path and mean free time of the states. We discuss as well the associated density matrix formalism.

### 4.1 Waves and wave packets

Consider the effective hamiltonian, eq.(3.48). As stated above, electroweak loops are irrelevant for the purpose of this section, in which case we could settle  $\omega_L^0 = \omega_R^0 = \omega_{QCD}^0$  (see eq.(3.23)). The  $L, R$  dichotomy will be relevant in the next section. The effective Dirac equation describing the quasi-particle interaction with the wall is:

$$i\partial_t\psi = H_{eff}\psi = \begin{pmatrix} -\frac{1}{3}i\sigma_z\partial_z - i\gamma + \omega_{QCD}^0 & \frac{m}{2}\theta(z) \\ \frac{m}{2}\theta(z) & \frac{1}{3}i\sigma_z\partial_z - i\gamma + \omega_{QCD}^0 \end{pmatrix}\psi. \quad (4.1)$$

There are many solutions to this differential equation. The problem to solve is the scattering of a quasi-quark hitting the wall from the unbroken phase. The initial conditions correspond then to a state localised on  $z < 0$  at its creation time, travelling towards the  $z > 0$  region, and with a mean free time and mean free path as described in subsection 3.3.

No single wave solution fulfills all these conditions. The gist of the problem is reflection, though, and waves damped in space and travelling towards the wall should be an appropriate heuristic treatment of the initial state, that we proceed to develop here. These solutions have then a mean free path (coherence length), but are eternal, that is, have no mean free time. All the initial conditions can be accounted for in term of wave packets instead, and we will see later that this physically more correct approach leads to the same conclusions.

An exponentially decaying wave, created in the unbroken phase at a point  $z_0 < 0$  within a mean free path ( $1/6\gamma$ ) away from the wall, and travelling towards  $z > 0$ , is given by

$$\psi_{inc}^\chi(z, t; \omega) = e^{-i\omega t} \theta(z - z_0) \left\{ \begin{aligned} &\theta(-z) \left[ e^{i\pi_\chi z} u_{\chi, \chi} + e^{-i\pi_{-\chi} z} r_\chi(\pi_\chi) u_{-\chi, \chi} \right] \\ &+ \theta(z) e^{i\pi_\chi^t z} [u_{\chi, \chi} + r_\chi(\pi_\chi) u_{-\chi, \chi}] \end{aligned} \right\}, \quad (4.2)$$

where  $\chi$  denotes chirality and  $u_{\chi, \sigma}$  is the normalised Dirac spinor for a particle with spin  $\sigma_z/2$  and chirality  $\chi$ .  $\pi_\chi$  is the incoming momentum of a particle with  $\sigma_z = \chi$ , i.e., positive group velocity

$$\pi_\chi = 3(\omega - \omega_\chi^0 + i\gamma) = p_\chi + 3i\gamma, \quad \pi_{-\chi} = 3(\omega - \omega_{-\chi}^0 + i\gamma), \quad (4.3)$$

where  $p_\chi = \text{Re}(\pi_\chi)$ .  $\pi_\chi^t$  is the corresponding transmitted momentum in the broken phase,

$$\pi_\chi^t = \frac{1}{2}(\pi_\chi - \pi_{-\chi}) + \frac{1}{2}\sqrt{(\pi_\chi + \pi_{-\chi})^2 - 9m^2}. \quad (4.4)$$

The reflection coefficient  $r_\chi(\omega)$  has the simple expression:

$$r_\chi(p_\chi) \equiv r_\chi(\omega) = -\frac{m/2}{p(\omega) + e^{i\phi}\sqrt{|p(\omega)^2 - m^2/4|}}, \quad (4.5)$$

with<sup>18</sup>

$$\phi = \frac{\arg(p(\omega) - m/2) + \arg(p(\omega) + m/2)}{2} \quad (4.6)$$

and

$$p(\omega) = \frac{1}{6} [p_\chi + p_{-\chi}] = \omega - \frac{\omega_\chi^0 + \omega_{-\chi}^0}{2}, \quad (4.7)$$

where we introduced the momentum-like variable  $p(\omega)$  to stress the analogy with the situation at  $T = 0$  [2]. The analytic continuation of  $r(p_\chi)$  to the complex plane for the variable  $p_\chi(\omega)$  is straightforward from eq. (4.5).

For quasi-quarks with current quark masses smaller than  $2\gamma$ ,

$$|r_\chi(\pi_\chi)| \equiv |r_\chi(\omega + i\gamma)| \leq \frac{m}{4\gamma}. \quad (4.8)$$

It follows that the reflection probability is suppressed for all flavours but the top. For the latter,  $|r(\omega)| \leq 1$ , as expected.

#### 4.1.1 Wave packets

Our main hypothesis results from the uncertainty principle. The finite life-time (and finite mean free path) of the quasiparticles induces a finite spreading of their energy (and momentum) spectrum of the order of  $2\gamma$  ( $6\gamma$ ). Wave packets allow a parametrisation of such a localisation in time and space. We use gaussian wave packets with a unique width  $1/d$ . Our final result will turn out to be independent of this particular choice of packets, the only requirement being  $d \leq 1/3\gamma$ .

Wave packet solutions to eq.(4.1) can be expressed as superposition of plane waves. Assume that, at time  $t_0$ , an incoming quasiparticle wave packet has been created around the position  $z_0 < 0$  in the unbroken phase, with a central momentum  $p_0$ :

$$\Psi_{inc}^\chi(z, t_0; z_0, t_0, p_0, d, \chi) = \sqrt{\frac{d}{2\pi^{3/2}}} \int_{-\infty}^{+\infty} dp e^{-d^2(p-p_0)^2/2} e^{ip(z-z_0)} u_{\chi,\chi}. \quad (4.9)$$

The choice of spinor with  $s_z = \chi$  ensures the positive group velocity, characteristic of an incoming wave. Notice that the eigenspinors of the Dirac Hamiltonian with positive group velocity are the same all over one branch of the spectrum (see fig. 2 (a)), as long as we stay in the unbroken phase and in the linear regime for the spectrum.

---

<sup>18</sup>To simplify the notations we use the same symbol  $r_\chi$  for the reflection coefficient as a function of  $\omega$  and as a function of  $p_\chi$ . The analytic behaviour of eq.(4.5) will be discussed later, see subsection 4.1.2.

From eq. (4.1) it is easy to derive the time evolution of the wave function (4.9), in the unbroken phase:

$$\begin{aligned}\Psi_{inc}^\chi(z, t; z_0, t_0, p_0, d, \chi) &= \\ &\theta(t - t_0) \sqrt{\frac{d}{2\pi^{3/2}}} \int_{-\infty}^{+\infty} dp_\chi e^{-d^2(p_\chi - p_0)^2/2} e^{ip_\chi(z - z_0)} e^{-i(\omega - i\gamma)(t - t_0)} u_{\chi, \chi} \\ &= \theta(t - t_0) \sqrt{\frac{1}{d\pi^{1/2}}} e^{-\frac{[(z - z_0) - 1/3(t - t_0)]^2}{2d^2}} e^{ip_0[(z - z_0) - 1/3(t - t_0)]} e^{-i\omega_\chi^0(t - t_0) - \gamma(t - t_0)} u_{\chi, \chi},\end{aligned}\quad (4.10)$$

where the relation between the incoming momentum,  $p_\chi$ , and  $\omega$  was given in eq. (4.3). Eq (4.10) exhibits the motion of the center of the packet with velocity  $1/3$ . The Fourier transform of eq.(4.10) is

$$\begin{aligned}\tilde{\Psi}_{inc}(p_\chi, t; z_0, t_0, p_0, d, \chi) &= \\ &\theta(t - t_0) \sqrt{\frac{d}{\pi^{1/2}}} e^{-d^2(p_\chi - p_0)^2/2} e^{-ip_\chi z_0} e^{-i(\omega - i\gamma)(t - t_0)} u_{\chi, \chi}.\end{aligned}\quad (4.11)$$

The wave function is normalised to 1 at  $t = t_0$ , and its norms decays exponentially as  $\sim e^{-2\gamma(t - t_0)}$  due to dissipation. Let us now turn to a statistical ensemble of particles. Consider, in the unbroken phase, an homogeneous flux of such wave packets travelling towards the wall. These particles “decay”, i.e. they are scattered, at a rate  $2\gamma$  during their flight. This decay must be exactly cancelled by creation at the same rate  $2\gamma$ , so that the equilibrium distribution of particles can remain stationary. To account for this effect, we introduce a continuous differential rate of creation  $N(z_0, t_0, p_0) dz_0 dt_0 dp_0$ . The density of incoming quasi-particles of chirality and spin  $\chi$  at some point  $z < 0$  *far from the wall* and at time  $t$  is given by

$$\begin{aligned}\Xi &= \int_{-\infty}^{+\infty} dp_0 \int_{-\infty}^t dt_0 \int_{-\infty}^{+\infty} dz_0 |\Psi_{inc}^\chi(z, t; z_0, t_0, p_0, d)|^2 N(z_0, t_0, p_0) \\ &= \frac{1}{2\gamma} \int_{-\infty}^{+\infty} dp_0 N(z_0, t_0, p_0).\end{aligned}\quad (4.12)$$

Taking for the rate of quasi-particle creation

$$N(z_0, t_0, p_0) = 2\gamma n_F(\omega_\chi^0 + p_0/3, T),\quad (4.13)$$

the equilibrium Fermi density is recovered,

$$\Xi = \int dp_0 n_F(\omega_\chi^0 + p_0/3, T),\quad (4.14)$$

where  $n_F(\omega) = 1/(\exp(\omega/T) + 1)$ .

#### 4.1.2 Reflection probability.

The reflected part of the wave packet, travelling backwards in the unbroken phase is

$$\Psi_{ref}^\chi(z, t; z_0, t_0, p_0, d) = \theta(t - t_0) \sqrt{\frac{d}{2\pi^{3/2}}} \int_{-\infty}^{+\infty} dp_\chi$$

$$e^{-d^2(p_\chi - p_0)^2/2} e^{-ip_\chi z - ip_\chi z_0} e^{-i(\omega - i\gamma)(t - t_0)} r_\chi(p_\chi) u_{-\chi, \chi}, \quad (4.15)$$

where the  $\omega$  dependence is the same than for  $\Psi_{inc}$ , as energy is conserved in the interactions with the wall, and where  $r_\chi(p_\chi)$  has been defined in eq. (4.5). In eq. (4.15),  $\chi$  ( $-\chi$ ) represents the incoming (outgoing) chirality.

Let us define the reflection probability  $n_r$  as the ratio of the reflected flux close to the wall on the unbroken side ( $z = 0^-$ ), to the incoming flux. Since the incoming and outgoing group velocities have the same absolute values, it amounts to the ratio between the reflected density at  $z = 0^-$  and the incoming density. Notice that the choice ( $z = 0^-$ ) maximises  $n_r$ , as the reflected flux will be diluted when travelling backwards in the unbroken phase. Further than a few mean free paths away from the wall, the reflected flux of particles is transported by *diffusion* rather than *free streaming*. As we will see in the next section, diffusion could be qualitatively described by replacing (4.13) with its local equilibrium generalisation. For simplicity, we concentrate now on the reflected flux close to the wall.

At time  $t = 0$ , the reflection probability is obtained integrating the reflected density, eq. (4.15), over all creation times in the past,  $t_0 < 0$ , and over all creation locations in the unbroken phase,  $z_0 < 0$ ,

$$n_r^\chi(z = 0, t = 0) = \frac{1}{\Xi} \int_{-\infty}^{+\infty} dp_0 \int_{-\infty}^0 dz_0 \int_{-\infty}^0 dt_0 N(z_0, t_0, p_0) \left| \Psi_{ref}^\chi(0, 0; z_0, t_0, p_0, d, \chi) \right|^2. \quad (4.16)$$

This is consistent with the creation probability eq. (4.12).  $N(z_0, t_0, p_0)$  was given in eq. (4.13).

The computation of the reflection probability, eq. (4.16), requires a careful analysis of the *mathematical* properties of the function  $r_\chi$ , eq. (4.5).  $r_\chi$  is analytic on the complex plane but for a cut extending on the real axis between  $p(\omega) = -m/2$  and  $p(\omega) = m/2$ . Close to the cut,  $\phi \simeq \pi/2$  in the upper half-plane, while  $\phi \simeq -\pi/2$  in the lower half-plane. When integrating on the real axis we will take the determination from the upper half-plane. Outside the cut on the real axis and for  $p(\omega) > m/2$ ,  $\phi = 0$  while for  $p(\omega) < -m/2$ ,  $\phi = \pi$ <sup>19</sup>. It results that  $|r_\chi(\omega)| \leq 1$ . More precisely,  $|r_\chi(\omega)| = 1$  for  $-m/2 < p(\omega) < m/2$ , and  $|r_\chi(\omega)| < 1$  outside that segment. This is illustrated in fig. (3). Fig (4) displays the phase of  $r_\chi(\omega)$ , and shows that it varies very fast over the real axis on the cut. It is worth to notice that this cut does correspond to the total reflection domain for plane waves. It is a very small domain for light quarks.

In eq. (4.15) the integral over  $p_\chi$  is strongly reduced by the rapid rotation of the phases of the exponential and the function  $r_\chi$ . This is at the origin of the dramatic suppression of CP asymmetry that we advocate in this paper. We have checked this suppression numerically, although the same result follows from a very simple analytic argument, which we proceed to develop. The only singularity in the integral  $dp_\chi$  in eq. (4.15) is the cut on the real axis of the function  $r_\chi$ . Consider a rectangle in the complex  $p_\chi$  plane with sides given by : the real axis, a parallel to it in the upper half-plane, and two vertical sides at  $\pm\infty$ . The extension of the integral in eq. (4.15) to this contour vanishes since no singularity is present inside the box. The integrals on the vertical sides vanish due to gaussian suppression. The integral in eq. (4.15) on the real axis can then be replaced by an integration on a parallel

---

<sup>19</sup>Then, on the real axis,  $r_\chi = m/2/(p(\omega) + \sqrt{p(\omega)^2 - m^2/4})$  for  $p(\omega) > m/2$ , and  $r_\chi = m/2/(p(\omega) - \sqrt{p(\omega)^2 - m^2/4})$  for  $p(\omega) < -m/2$ .

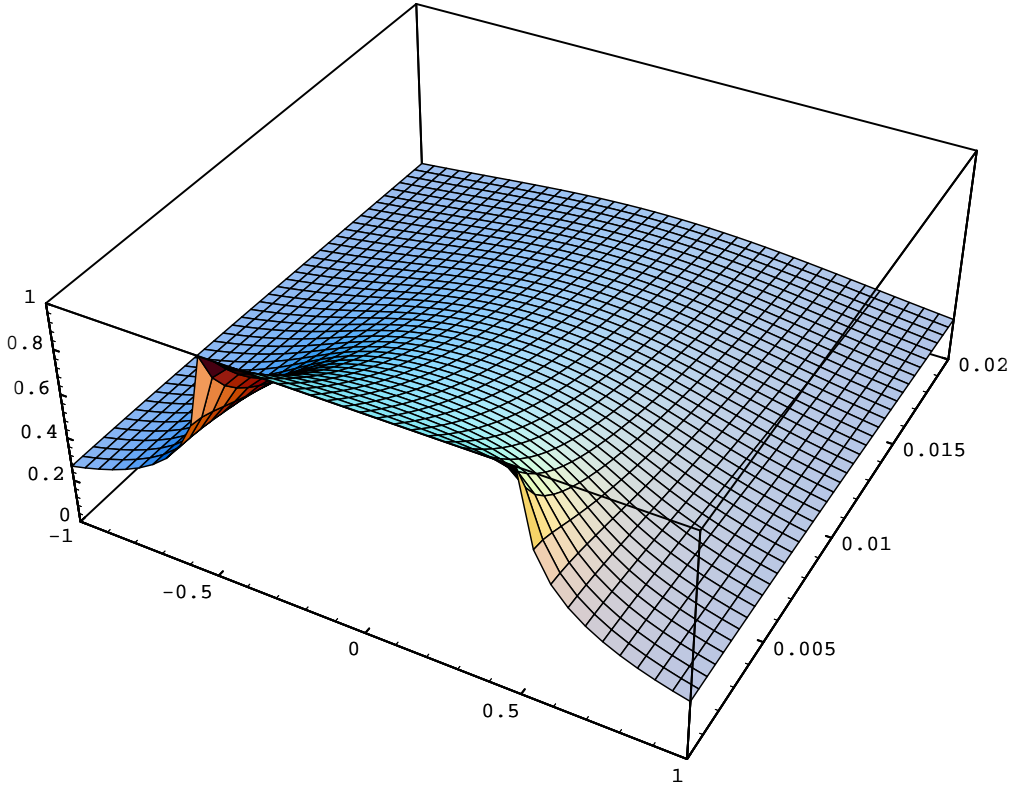


Figure 3: Plot of  $|r(p)|$  on the upper complex  $p(\omega)$  half-plane, with  $m = 0.5$ . The lower left edge is the real axis. The crest at  $|r(p)| = 1$  on this axis corresponds to total reflection. Notice the rapid decrease of  $|r(p)|$  with increasing imaginary part.

axis,  $\int_{-\infty+3i\beta\gamma}^{\infty+3i\beta\gamma} dp_\chi$ , with  $0 \leq \beta \leq 1$ . The condition  $\beta \geq 0$  ensures that the integral over  $z_0$  in (4.16) is finite, while the condition  $\beta \leq 1$  does the same for the integral over  $t_0$ .

The choice  $\beta = 1$ , and thus  $\text{Im}(p_\chi) = 3i\gamma$  is equivalent to change variables  $p_\chi \rightarrow p_\chi + 3i\gamma$  in eq. (4.15)<sup>20</sup>:

$$\Psi_{ref}^\chi(z, t; z_0, t_0, p_0, d) = \theta(t - t_0) \sqrt{\frac{d}{2\pi^{3/2}}} \int_{-\infty}^{+\infty} dp_\chi e^{-d^2(\pi_\chi - p_0)^2/2} e^{-i\pi_\chi z - i\pi_\chi z_0} e^{-i\omega(t-t_0)} r_\chi(\pi_\chi) u_{-\chi, \chi}. \quad (4.17)$$

The reflection coefficient  $r_\chi(\pi_\chi)$  is then bounded as displayed in eq. (4.8). The exponential in (4.15) also provides a factor  $\exp(9d^2\gamma^2/2)$ , and a bound for  $\Psi_{ref}^\chi$  results as long as  $d \ll 1/\gamma$ <sup>21</sup>,

$$\left| \Psi_{ref}^\chi(z, t; z_0, t_0, p_0, d) \right| \leq \frac{m}{4\sqrt{p(\omega_\chi^0 + p_0/3)^2 + \gamma^2 + O(m^2)}} + O(3d\gamma), \quad (4.18)$$

where  $p(\omega)$  has been defined in (4.7) and the bound in (4.8) has been slightly improved for later use.

<sup>20</sup>Notice that  $p_\chi + 3i\gamma$  is the variable  $\pi_\chi$  defined in eq. (4.3).

<sup>21</sup>Physically, this inequality means that the layer of particles sitting “on” the wall has a negligible thickness  $d$ , compared with the layer of particles that ever have a chance to reach the wall before being damped.

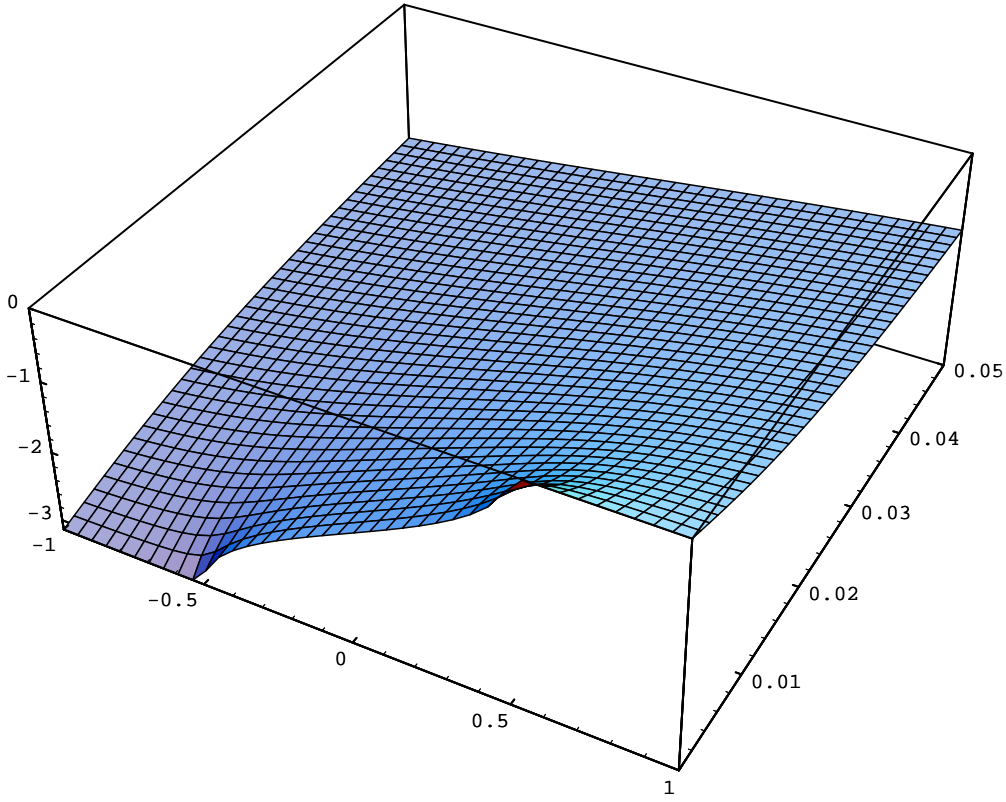


Figure 4: Plot of the phase of  $r(p)$  on the upper complex  $p(\omega)$  half-plane, with  $m = 0.5$ . The phase is zero on the real axis outside the total reflection domain,  $-0.5 < x < 0.5$ , and varies rapidly inside this domain. This explains the suppression observed when the integration is performed on the real axis.

From eq. (4.16) it follows that

$$n_r(0,0) \leq \frac{m^2}{16\sqrt{\gamma^2 + O(m^2)}\Xi} \quad (4.19)$$

It is worth to notice that the results expected for zero damping rate  $\gamma = 0$  can be recovered. In this case, eq. (4.19) reduces to

$$n_r(0,0) \sim \frac{m}{\Xi}, \quad (4.20)$$

This is indeed the result that would follow directly for vanishing damping rate, when the reflection probability can be directly computed in terms of plane waves:

$$\frac{1}{\Xi} \int dp_\chi n_F(\omega, T) |r_\chi(\omega)|^2 \sim \frac{m}{\Xi} \quad (4.21)$$

where  $\omega$  and  $p_\chi$  are related as in eq. (4.7).

The comparison of eqs (4.19) and (4.20) shows a  $\sim m/(16\gamma)$  suppression of the reflection probability when the damping rate is taken into account, due to the fast rotation of the phases in the integral in eq. (4.15). This is a typical quantum effect: the different frequencies in the integral, eq. (4.15), add up as waves, not as probabilities. We may express the phenomenon at work as follows: the damping rate destroys the quantum coherence which is necessary to have a large reflection probability, through an average over a rapidly rotating phase,

$$\langle r_\chi \rangle \ll \langle r_\chi^\dagger \rangle \ll \langle |r_\chi|^2 \rangle. \quad (4.22)$$

The spread in energy and momentum of the quasi-particles results in a smearing of the reflection integrals, contrary to the case of vanishing damping rate, where the states are monochromatic, and thus well represented by plane waves.

### 4.1.3 A simple approximation to the reflection probability.

A useful simplification is obtained if the integration on  $t_0$  in eq. (4.16) is extended to  $+\infty$ . A qualitative estimate of the error introduced by this trick is given here. A rigorous proof is developed in appendix A.

The presence of the potentially dangerous exponential  $e^{\gamma t_0}$  in the expression for  $\Psi_{ref}$ , eq. (4.15), does not lead to any divergence, due to the gaussian smearing. Indeed, the only effect of extending the  $t_0$  integration from 0 to  $+\infty$  is to add a gaussian tail. The width of the gaussian being  $d$ , the added tail will be  $O(\exp(-1/(\gamma d)^2))$ , i.e. small as long as  $d\gamma \ll 1$ . More precisely, as explained in appendix A, the correction is negligible for

$$3d\gamma \ll 1. \quad (4.23)$$

The reflection probability (4.16) is then given by

$$n_r^\chi(0, 0) = \frac{2\gamma}{\Xi} \int_{-\infty}^{+\infty} dp_0 \int_{-\infty}^0 dz_0 \int_{-\infty}^{\infty} dt_0 n_F(\omega_\chi^0 + p_0/3, T) \frac{d}{2\pi^{3/2}} \int_{-\infty}^{\infty} dp_\chi \int_{-\infty}^{\infty} dp'_\chi e^{-d^2(\pi_\chi - p_0)^2/2 - d^2(\pi'_\chi - p_0)^2/2} e^{i\pi'_\chi z_0 - i\pi_\chi z_0} e^{i(\omega - \omega')t_0} r_\chi(\pi_\chi) r_\chi^*(\pi'_\chi). \quad (4.24)$$

The integral over  $t_0$  simply gives  $2\pi\delta(\omega - \omega') = 6\pi\delta(p_\chi - p'_\chi)$ . The  $z_0$  dependence is then  $\exp(-6\gamma z_0)$ , whose integral is trivial. Finally,

$$n_r^\chi(0, 0) = \frac{1}{\Xi} \int_{-\infty}^{+\infty} dp_0 n_F(\omega_\chi^0 + p_0/3, T) \frac{d}{\sqrt{\pi}} \int_{-\infty}^{\infty} dp_\chi e^{-d^2(p_\chi - p_0)^2 + (3d\gamma)^2} |r_\chi(\pi_\chi)|^2. \quad (4.25)$$

This is the main result of this section. After neglecting the  $t_0 > 0$  terms and *upon the change of variables*  $p_\chi \rightarrow p_\chi + 3i\gamma$  *and correspondingly*  $\omega \rightarrow \omega + i\gamma$ , the reflected flux for wave packets is just a gaussian smear-out of the reflection fluxes for plane waves, as naively expected.

Two comments are appropriate. The first one concerns particle number, which must be conserved. Unitarity implies that the damping of reflected flux is exactly compensated by the enhancement of the transmitted one. The underlying physics can also be understood. A very localised particle penetrates the broken phase in a time  $1/3d$ , whereas for small masses it requires a rather long time  $2/m$  to be significantly reflected (the reflection dominantly happens in an energy window of gap  $\sim m$ , the total reflection domain, and by uncertainty principle this corresponds to a time  $\sim 1/m$ ). If in between the particle is “measured” in the broken phase by collisions with the plasma, the wave function collapses into one corresponding to a localised particle in the broken phase, and as a result, the particle has been effectively transmitted.



Secondly, the  $d$  dependence of (4.15) can be clarified. When the mass is large enough,  $\gamma \ll 1/(3d) \ll m/2$ , reflection typically occurs between 2 collisions, and the effect of both the  $\gamma$ -shift and the  $1/(3d)$ -smearing can be neglected, nicely recovering the usual asymptotic reflection probability for plane waves. For the opposite limit of small masses, the  $d$  dependence can also be mild. Indeed, exchanging the order of integration in (4.25) leaves us with a thermal average of the reflection probabilities  $|r_\chi(\pi_\chi)|^2$ , according to an effective thermal distribution

$$n_F^d(\omega_\chi^0 + p_\chi/3, T) = \frac{d}{\sqrt{\pi}} \int_{-\infty}^{\infty} dp_0 e^{-d^2(p_\chi - p_0)^2 + (3d\gamma)^2} n_F(\omega_\chi^0 + p_0/3, T). \quad (4.26)$$

If  $n_F$  is smooth on scales  $1/(3d)$  (as is the case, close to equilibrium, if  $1/(3d) \ll T$ ),  $n_F^d \sim n_F$  and the average (4.25) is close to a thermal average of monochromatic reflection probabilities.

We have checked numerically this  $d$  independence of our result. If the distribution probability was arbitrary and far from equilibrium (i.e. far from  $n_F(\omega)$ ), our linear response approach to the relaxation processes loses its meaning, and finer knowledge of all relaxation processes becomes necessary. Let us thus stress that we assumed the quasi-particle distributions to be close to equilibrium (and effectively reducing the reflection coefficient makes this assumption easier to meet, for a given wall speed), and moreover required

$$\gamma \ll \frac{1}{3d} \ll T \Leftrightarrow g_s^2 T \ll \frac{1}{3d} \ll T, \quad (4.27)$$

which is always satisfied for weak coupling  $g_s \ll 1$ . Our model for decoherence accounts for the physical consequences of a non-vanishing damping rate. In real QCD  $g_s$  is not small, and we believe that a more realistic treatment would lead to a further suppression of the CP-asymmetry than advocated in this paper. Indeed, as the damping rate increases the description of the system in terms of quasi-particle ( an essential ingredient of the approach) loses its physical meaning.

## 4.2 Density matrix.

In this subsection, the results of the preceding one are reproduced using the formalism of density matrices. The language of density matrices is very convenient for plasma physics. It will clarify how the suppression effect found above depends on the quantum aspects of the density matrix, and their relation with the breaking of thermal equilibrium in the process under study.

The effective Hamiltonian in the plasma rest frame, eq. (4.1), can be split into hermitian and non-hermitian parts:

$$H_{eff} \equiv H_{herm} - i\gamma. \quad (4.28)$$

We consider the reduced density matrix  $\rho$  for one quasi-particle at equilibrium in the unbroken phase. It obeys the following Boltzman equation,

$$\partial_t \rho(t) = -i[H_{herm}, \rho(t)] + G - L. \quad (4.29)$$

$G$  ( $L$ ) is a gain (loss) term corresponding to the creation (disappearance) of quasiparticles due to collisions with the medium. To simplify the problem, we used a linearised equation. In

this approximation, the  $L$  term is related to the damping rate by  $L = -2\gamma\rho$ . At equilibrium, the probability loss due to  $L$  must be compensated by the  $G$  term. However, and this is our essential assumption,  $G$  creates quasi-particles from the medium which are out of phase with respect to the ones destroyed by  $L$ . We further assume  $G$  to be homogeneous in space and time in the unbroken phase. A simple example is given by the creation rate defined in eqs. (4.12)-(4.13). The resulting equation for the reduced density matrix of a quasi-particles with positive group velocity (incoming) and chirality  $\chi$ , is then given by:

$$\begin{aligned} \partial_t \rho(p, p'; t) + i[H_{herm}, \rho(p, p'; t)] &= -2\gamma\rho(p, p'; t) + \frac{1}{\Xi L} \int dz_0 \theta(-z_0) \\ \int_{-\infty}^{+\infty} dp_0 N(z_0, t, p_0) \tilde{\Psi}_{inc}(p, t; t, p_0, z_0, d, \chi) \tilde{\Psi}_{inc}^\dagger(p', t; t, p_0, z_0, d, \chi). \end{aligned} \quad (4.30)$$

$\Xi$  has been defined in eq. (4.12),  $L$  is the volume of the one dimensional box in which the density matrix is normalised, and the  $\theta(-z_0)$  factor in the inhomogeneous term accounts for quasiparticle creation in the unbroken phase.  $\Psi_{inc}$  was defined in eqs. (4.9)-(4.11). The solution of eq. (4.30) is

$$\begin{aligned} \rho(p, p'; t) &= \frac{2\gamma}{\Xi L} \int dz_0 dt_0 dp_0 \theta(-z_0) \theta(t - t_0) n_F(\omega^0 + \chi p_0/3, T) \\ &\tilde{\Psi}_{inc}(p, t; t_0, p_0, z_0, d, \chi) \tilde{\Psi}_{inc}^\dagger(p', t; t_0, p_0, z_0, d, \chi), \end{aligned} \quad (4.31)$$

where eq. (4.13) has been used. From eq. (A.7) in appendix A and eq. (4.14) it follows that

$$\int dp \text{Tr}[\rho_\chi^u(p, p)] = 1. \quad (4.32)$$

It is possible to see that eq. (4.31) reduces to the equilibrium distribution in the absence of the wall, i.e., when the factor  $\theta(-z_0)$  is taken off. Integrating then  $z_0$  from  $-\infty$  to  $+\infty$  yields a  $2\pi\delta(p - p')$  factor, consistent with translation invariance in the absence of a wall, and  $\rho$  becomes diagonal in momentum as expected. The  $t_0$ -integral cancels the  $2\gamma$  factor in eq. (4.31),

$$\rho(p, p'; t) = \frac{2\pi\delta(p - p')}{\Xi L} \int dp_0 n_F(\omega_\chi + p_0/3, T) \frac{e^{-d^2(p-p_0)^2}}{\pi^{1/2}/d}. \quad (4.33)$$

In the infinite volume limit,  $2\pi\delta(0) \simeq L$ , and the  $p_0$  integral gives a gaussian smearing of the equilibrium distribution,

$$\rho(p, p; t) = \frac{1}{\Xi} \int dp_0 n_F(\omega_\chi + p_0/3, T) \frac{e^{-d^2(p-p_0)^2}}{\pi^{1/2}/d} \simeq \frac{n_F(\omega, T)}{\Xi} \quad dT \gg 1 \quad (4.34)$$

since the smearing can be neglected for  $d$  large enough, i.e.

$$T \gg \Delta E = \frac{dE}{dp_0} \Delta p_0 \sim \frac{1}{3d}, \quad (4.35)$$

which is the usual condition (4.23), (4.27), and the Fermi equilibrium distribution is obtained.

In the present problem, the wall at  $z = 0$  requires to treat separately the  $z_0 < 0$  and  $z_0 > 0$  regions, though. Only the first one is involved in describing the incoming flux, and the

$z_0$  integration in eq. (4.31) provides an extra non-diagonal piece arising from the principal part of  $1/(p - p')$ . This term is exponentially suppressed when  $|p - p'| > 1/d$ , as (4.11) imposes that both  $p$  and  $p'$  lie within a distance  $1/d$  from some  $p_0$ .  $1/d$  is then an upper bound for the non-diagonality of  $\rho$ . Depending on the shape and height of the wall, the  $z_0 > 0$  contribution may ultimately reduce the maximum  $|p - p'|$ , as it was shown above when the wall was removed. This non diagonality of  $\rho$  is a quantum effect<sup>22</sup> as is manifest in the oscillation of the  $\exp(-i(p - p')(t - t_0)/3)$  factor present in (4.31), through (4.11) and (4.7).

A simpler way to describe the effect follows by computing the Fourier transform of  $\rho$  with respect to  $(p - p')$ , in order to obtain the Wigner function  $f(p, z)$  [23]. A sharp cutoff imposed in  $z_0$  then translates into inhomogeneities of  $f(z, p)$  on scales at least bigger than  $d$ , the individual particle diameter. The fact that  $f(z, p)$  is not a real positive function (as it would be in the semiclassical limit) is a sign of quantum effects.

#### 4.2.1 Reflection probability from the density matrix.

The thermal average of any physical observable  $O$  is given by  $\text{Tr}(\rho O)/\text{Tr}(\rho)$ . In particular, the reflection probability is the thermal average of  $r_\chi(p_\chi)r_\chi^*(p'_\chi)$ , with  $r_\chi(p_\chi)$  as defined in (4.5). For a diagonal density matrix, i.e. in the absence of quantum coherence, the reflection probability amounts to the average of  $|r_\chi(p_\chi)|^2$ , and this is what happens for vanishing damping rate (see the discussion in subsection (4.1.2)).

The density of incoming particles at position  $z < 0$  is given in terms of the density matrix by

$$d^{inc}(z) = \frac{1}{2\pi} \int \int dpdp' e^{i(p-p')z} \rho(p, p') = \frac{1}{L} \quad \text{if } 0 < -\frac{z}{d} \ll 1. \quad (4.36)$$

In fact  $d^{inc}(z)$  depends only slightly on  $z$  when  $3\gamma d \ll 1$ :

$$d^{inc}(0) = \frac{\Xi^{wall}}{L\Xi} \simeq \frac{1}{L} \quad \text{if } 3\gamma d \ll 1, \quad (4.37)$$

as can be seen from eqs (A.7) and (A.9) in appendix A. For the problem under study, with a non diagonal density matrix, the reflection probability is given by the ratio of the density of reflected particles over the incoming density, i.e.

$$n_r = \frac{L}{2\pi} \int dpdp' \rho(p, p'; t = 0) r(p) r^\dagger(p'), \quad (4.38)$$

where time translational invariance was used to choose  $t = 0$ . As expected, eq. (4.38) is equivalent to (4.16) and the calculation will proceed exactly as in the preceding subsections.

## 5 Several flavours: CP violation.

In this section, we include the non-diagonal weak contributions to the effective Hamiltonian in a perturbative expansion. We then compute the CP-asymmetry and compare our results with existing literature.

---

<sup>22</sup>A diagonal density matrix is just a probability distribution, i.e. it is purely classical, it exhibits no quantum coherence.

## 5.1 Effective Hamiltonian

Only the quarks with the same charge are mixed, and the Hamiltonian will be factorised for down and up sectors. In section (3), we found the effective unperturbed Hamiltonian (3.51) in the case of several generations, which we recall here:

$$H_{eff}^0 = \begin{pmatrix} -\frac{1}{3}i\sigma_z\partial_z - i\gamma + \hat{\omega}_R^0 & \frac{m}{2}\theta(z) \\ \frac{m}{2}\theta(z) & \frac{1}{3}i\sigma_z\partial_z - i\gamma + \hat{\omega}_L^0 \end{pmatrix}. \quad (5.1)$$

It contains only the leading  $T$ , QCD and flavour diagonal electroweak corrections. It has been linearised in momentum. In order to obtain an observable asymmetry, the remaining corrections, i.e. the non-diagonal weak corrections and those subleading in  $T$ , are essential ingredients. The full effective hamiltonian is

$$H_{eff} = H_{eff}^0 + \theta(-z)\delta H_{eff}^u + \theta(z)\delta H_{eff}^b, \quad (5.2)$$

where

$$\delta H_{eff}^{u,b} = \frac{1}{2} \begin{pmatrix} [\delta h_R^{u,b}(\omega, k) - i\delta a_R^{u,b}(\omega, k)\sigma_z\partial_z] & \frac{1}{2}mc(\omega, k)\theta(z) \\ \frac{1}{2}mc(\omega, k)\theta(z) & [\delta h_L^{u,b}(\omega, k) + i\delta a_L^{u,b}(\omega, k)\sigma_z\partial_z] \end{pmatrix}. \quad (5.3)$$

$\delta h^{u,b} = h^{u,b} - \bar{h}$  and  $\delta a^{u,b} = a^{u,b} - \bar{a}$  are flavour dependent and non-diagonal, as defined and discussed in subsections (3.1.2), (3.2.1) and (3.2.2). They have to be also linearised in momentum. To be consistent with our approximation (i.e. that these effects do not modify the residues derived from the free hamiltonian (3.48)) we must expand these functions around the poles (3.31) and take only the zero order. This means that corrections of  $O(k\delta h, a, c)$  are neglected, which is a reasonable assumption for the low momentum region we are considering.

Finally, the hamiltonian we must consider is:

$$H_{eff} = H_{eff}^0 + \frac{1}{2}\theta(-z) \begin{pmatrix} \delta h_R^u(\omega^0, 0) & 0 \\ 0 & \delta h_L^u(\omega, 0) \end{pmatrix} + \frac{1}{2}\theta(z) \begin{pmatrix} \delta h_R^b(\omega^0, 0) & mc(\omega^0, 0) \\ mc(\omega^0, 0) & \delta h_L^b(\omega^0, 0) \end{pmatrix}, \quad (5.4)$$

where we can take  $\omega^0 = \omega_{QCD}^0$ , i.e., it contains just the dominant QCD part. The precise choice of  $\omega^0$  in the arguments of the perturbed functions only influences subdominant contributions to the asymmetry.

## 5.2 Reflection Matrix and CP-Asymmetry

We are now ready to compute the CP-asymmetry defined in Sec. 2, eq. (2.10),

$$\Delta_{CP} = \frac{L}{2\pi} \text{sign}(\chi) \int \int dp dp' [\rho \text{Tr}\{r_{-x}^u \dagger r_{-x}^u - (\bar{r}_x^u)^\dagger \bar{r}_x^u\}]. \quad (5.5)$$

Being a CP-odd asymmetry it must contain the contribution of CP-violating phases, for which at least three generations are needed. In this case, the reflection and transmission amplitudes  $r, t$  are  $3 \times 3$  matrices in flavour space.

We show below that an effect is present at order  $\alpha_W^2$  in rate, through subleading  $T$  corrections. At leading order in  $T$ ,  $O(T^2)$ , there is no contribution at this electroweak order,

because the only flavour dependence is through Yukawa couplings. The physical reason is CKM unitarity. The order  $\alpha_W^2$  effect is tantamount to a one-loop electroweak correction in the amplitudes. Denote by  $i$  and  $f$  the external initial and final flavours, and  $l$  (or  $l'$ ) the internal one in the loop. Convoluting two of these diagrams gives a contribution to the rate  $\propto \text{Im}\{K_{lf}^* K_{li} (K_{l'f}^* K_{l'i})^*\}$ . If the function accompanying this factor contains no antisymmetric dependence on the internal flavours, the contribution will vanish when the sum over  $l$  and  $l'$  is performed. At leading order in  $T$ , the dependence on Yukawa couplings is insufficient to produce a non-zero effect, because they factorise as a symmetric function of  $l, l'$ .  $\Delta_{CP}$  would then be a higher order electroweak effect, i.e.,  $\alpha_W^3$ . Subleading  $T$  corrections do contain an explicit internal quark mass dependence, which results in the above mentioned antisymmetric functions.

In section 4, we have shown that the reflection probability of quasi-particles in a single flavour world can be written as a gaussian smear-out of the reflection probability for plane waves (with zero damping rate) after making an analytic continuation  $p_\chi \rightarrow p_\chi + 3i\gamma$ , eq. (4.25). This result holds as well in the case of several generations:

$$n_r^\chi(0, 0) = \frac{1}{\Xi} \int_{-\infty}^{+\infty} dp_0 n_F(\omega_\chi^0 + p_0/3, T) \frac{d}{\sqrt{\pi}} \int_{-\infty}^{\infty} dp_\chi e^{-d^2(p_\chi - p_0)^2 + (3d\gamma)^2} \text{Tr}[r_\chi(\pi_\chi) r_\chi^\dagger(\pi_\chi)], \quad (5.6)$$

where now  $r_\chi(\pi_\chi)$  are  $3 \times 3$  matrices and  $\text{Tr}$  refers to the tracing over the flavour indices. The problem is then reduced to calculate the reflection matrices for plane waves  $r_\chi(p_\chi) = r_\chi(\omega)$ , evaluate them in the complex point  $\pi_\chi$  and, finally, perform the gaussian and thermal averages.

Let us start by computing  $r_\chi(\omega)$ . For  $\delta h = 0$ , the problem reduces to three independent one-flavour cases, whose solution we know, eq. (4.5). An analytic expression in the case of the simplified effective Hamiltonian, eq. (5.4), is still too difficult to find. We will use a perturbative approach to obtain an analytic result. The procedure involves deriving an exact equation for the reflection amplitude, and proceeding then by iteration, in powers of  $\delta h_{L,R}$ . This corresponds to an expansion of the asymmetry (2.10) in  $\alpha_w \sin\theta_c$ , as the CP-violating effects are contained in the non-diagonal weak terms.

We work in the flavour basis that diagonalises the unbroken effective Hamiltonian,  $H_{eff}^u$ . The transformation to this basis from the one corresponding to the unperturbed Hamiltonian,  $H_{eff}^0$ , has the form

$$\psi \equiv \begin{pmatrix} \psi^R \\ \psi^L \end{pmatrix} = \begin{pmatrix} I_3 & 0 \\ 0 & O_L \end{pmatrix} \begin{pmatrix} \psi'^R \\ \psi'^L \end{pmatrix} \equiv O\psi', \quad (5.7)$$

where  $\psi^\chi$  are spinors with three flavour components,  $I_3$  is the identity matrix and  $O_L$  is a unitary  $3 \times 3$  matrix. In the prime basis, the solution for right quasiparticle with energy  $\omega$  coming from the unbroken phase has the usual form (4.2):

$$\psi_{inc}^{\prime\chi}(z, t; \omega) = e^{-i\omega t} \left\{ \begin{aligned} &\theta(-z) [e^{ip_\chi z} u_{\chi,\chi} + e^{-ip_\chi z} r_\chi(p_\chi) u_{-\chi,\chi}] \\ &+ \theta(z) e^{ip_\chi^\dagger z} [u_{\chi,\chi} + r_\chi(p_\chi) u_{-\chi,\chi}] \end{aligned} \right\}, \quad (5.8)$$

where  $p_\chi$  is the incoming particle momentum as defined in eq. (4.3).

It is possible to obtain an implicit equation for  $r_R$  and  $r_L$  by imposing,

$$z > 0 \quad O^\dagger H_{eff}^b O \psi' = \omega \psi'. \quad (5.9)$$

For an incoming right-handed quark, eq. (5.9) gives

$$\begin{aligned} r'_R [\hat{\omega}_R^0 - \omega + \frac{1}{2} \delta h_R^b(\omega^0)] + [\hat{\omega}_L^0 - \omega + \frac{1}{2} \delta h_L^b(\omega^0)] r'_R \\ + \frac{1}{2} r'_R [1 - c(\omega^0)] m r'_R + \frac{1}{2} m [1 - c(\omega^0)]^\dagger = 0, \end{aligned} \quad (5.10)$$

where  $r'_R \equiv O_L r_R$ . As  $O_L$  is unitary,  $\Delta_{CP}$  is unchanged upon replacing  $r \rightarrow r'$ .

In the same way, the equation for antiparticles reads

$$\begin{aligned} \bar{r}'_R [\hat{\omega}_R^0 - \omega + \frac{1}{2} (\delta h_R^b(\omega^0))^*] + [\hat{\omega}_L^0 - \omega + \frac{1}{2} (\delta h_L^b(\omega^0))^*] \bar{r}'_R \\ + \frac{1}{2} \bar{r}'_R [1 - c(\omega^0)^*] m \bar{r}'_R + \frac{1}{2} m [1 - c(\omega^0)^*]^\dagger = 0. \end{aligned} \quad (5.11)$$

A similar equation for  $L$  reflection amplitudes can be written, although it is not needed to compute  $\Delta_{CP}$ .

We look for a perturbative solution of equations (5.10) and (5.11) in powers of  $\alpha_w$ :

$$r_R = r_R^{(0)} + r_R^{(1)} + r_R^{(2)} + \dots \quad (5.12)$$

$r_R^0$  is then the solution in the limit  $\delta h, \delta a, c = 0$  and it reduces to (4.5), as expected. To lighten the notation, we will skip the subindices  $R$  on  $r$ 's from now on. The first and second orders are given by

$$r_{ij}^{(1)} = -\frac{1}{2} \frac{(r^{(0)} \delta h_R^{b(1)} + \delta h_L^{b(1)} r^{(0)} - r^{(0)} \delta c^{(1)} m r^{(0)} - m \delta c)_{ij}}{d_{ij}} \quad (5.13)$$

and

$$\begin{aligned} r_{ij}^{(2)} = & -\frac{1}{2} \frac{(r^{(1)} \delta h_R^{b(1)} + \delta h_L^{b(1)} r^{(1)} - r^{(1)} \delta c^{(1)} m r^{(0)} - r^{(0)} \delta c^{(1)} m r^{(1)})_{ij}}{d_{ij}} \\ & -\frac{1}{2} \frac{(r^{(1)} m r^{(1)} + r^{(0)} \delta h_R^{b(2)} + \delta h_L^{b(2)} r^{(0)} - r^{(0)} \delta c^{(2)} m r^{(0)} - m \delta c^{(2)})_{ij}}{d_{ij}}, \end{aligned} \quad (5.14)$$

where the indices refer to flavour and  $d_{ij} \equiv (\omega_L^i + \omega_R^j - 2\omega) + \frac{m_i r_{ii}^0}{2} + \frac{m_j r_{jj}^0}{2}$ .

It follows from the discussion in subsection 4.1 that  $r^0$  are complex in the region of total reflection, and this region is the same for particles and antiparticles. This gives rise to CP-even phases. In order to generate an observable CP-asymmetry, they must interfere with the CKM one, contained in the non-diagonal weak corrections:  $\delta h_R^b, \delta h_L^b, c$ . Using eq. (3.11), and neglecting those terms in  $\delta h_L$  that have the same dependence on internal masses (or

Yukawa couplings) than  $\delta h_R$ , because they give a zero contribution at this order, we can easily obtain:

$$\delta h_R^b = \alpha_w \lambda_i \lambda_f \sum_l K_{li} K_{lf}^* I_R(M_l^2), \quad \delta h_L^b = \alpha_w \sum_l K_{li} K_{lf}^* I_L(M_l^2) \quad (5.15)$$

and

$$c = \frac{\lambda_f}{m_i} \sum_l K_{li} K_{lf}^* I_m(M_l^2), \quad (5.16)$$

where we have defined

$$I_R(M_l^2) = -\frac{\pi}{2} H(M_l, M_W), \quad I_L(M_l^2) = \lambda_l^2 I_R(M_l^2), \quad I_m(M_l^2) = \pi \lambda_l M_l C(M_l, M_W). \quad (5.17)$$

It then follows that the first effect in the asymmetry appears at  $O(\alpha_w^2)$  and it comes only from the interference of the  $O(\alpha_w)$  effects in  $\delta h_R^b$  and  $\delta h_L^b$ . Consequently, there is no effect at  $O(\alpha_w)$  at leading order in  $T$ , because at this order  $\delta h_R^b = 0$ . It is interesting to analyze the expression for the non-integrated asymmetry at this order, where the GIM mechanism is explicitly operative:

$$\begin{aligned} \Delta_{CP}^{(2)} &\equiv Tr [ r^{(1)\dagger} r^{(1)} + r^{(2)\dagger} r^{(0)} + r^{(0)\dagger} r^{(2)} - \text{antiparticles} ] \\ &\sim \sum_{i,j} Im [ \delta h_L^b ]_{ji} \delta h_R^b ]_{ij} \times Im \left\{ r_{ii}^{0*} \left[ \frac{r_{jj}^0}{|d_{ij}|^2} + \frac{m_j ((r_{ii}^0)^2 - (r_{jj}^0)^2)}{2d_{ii}d_{ij}d_{ji}} + \frac{r_{jj}^0}{d_{ii}} \left( \frac{1}{d_{ij}} + \frac{1}{d_{ji}} \right) \right] \right\}. \end{aligned} \quad (5.18)$$

$\Delta_{CP}^{(2)}$  can be shown to have the following structure:

$$\Delta_{CP}^{(2)} \sim \alpha_w^2 (2iJ) T^{int} T^{ext}, \quad (5.19)$$

where  $J$ ,  $T^{int}$  and  $T^{ext}$  contain the expected “à la Jarlskog” behaviour of the asymmetry as a function of the weak angles ( $J$ ), the internal quark ( $T^{int}$ ) and the external quark masses ( $T^{ext}$ ). The connection between (5.18) and (5.19) is

$$\begin{aligned} Im [ \delta h_L^b ]_{ji} \delta h_R^b ]_{ij} &= \alpha_w^2 \lambda_i \lambda_j 2i \sum_{l,l'} Im [ K_{li} K_{lj}^* K_{l'j} K_{l'i}^* ] (\lambda_l^2 - \lambda_{l'}^2) I_R(M_{l'}^2) I_R(M_l^2) \\ &\equiv \alpha_w^2 \lambda_i \lambda_j (\pm 2iJ) T^{int}, \end{aligned} \quad (5.20)$$

with

$$J \equiv \pm Im [ K_{li} K_{lj}^* K_{l'j} K_{l'i}^* ] = c_1 c_2 c_3 s_1^2 s_2 s_3 s_\delta,$$

and

$$T^{int} \equiv \sum_l (\lambda_l^2 - \lambda_{l+1}^2) I_R(M_l^2) I_R(M_{l+1}^2). \quad (5.21)$$

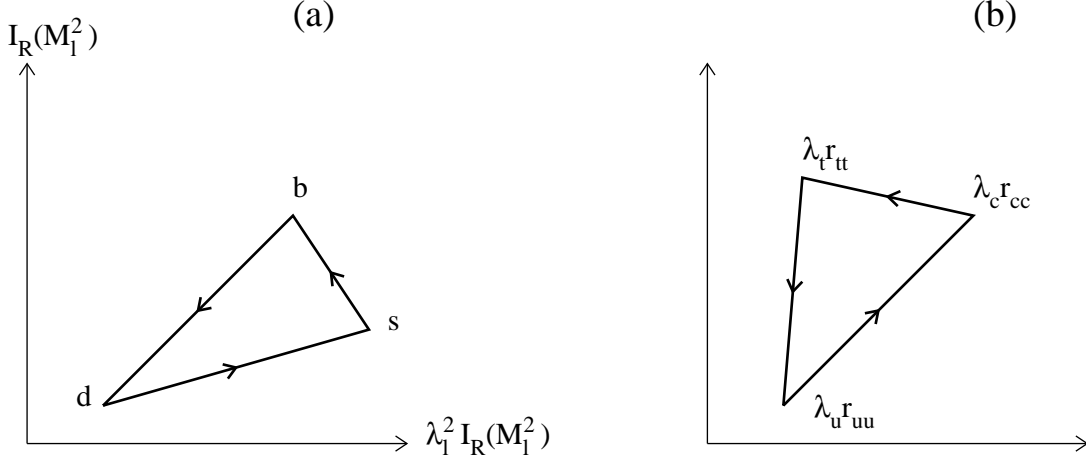


Figure 5: (a) The triangle in the complex plane, with area  $T^{int}$ . (b) The triangle in the complex plane, with area  $T^{ext}$ . In both cases, the sign is negative (positive) if the arrows turn (anti)-clockwise. This figure is only illustrative, a realistic triangle would look extremely flat due to the huge mass hierarchy between quark masses.

The  $\pm$  sign in  $J$  refers to the cyclic order of  $i, j$  and  $l + 1$  must be understood as modulo 3.  $T^{int}$  is the oriented area of the triangle formed by the three points in the complex plane given by  $\lambda_l^2 I_R(M_l^2) + i I_R(M_l^2)$ , corresponding to the three flavours of the internal quarks:  $l = 1, 2, 3$ , shown in fig. (5 (a)) From this construction, it is obvious that the triangle would collapse into a line whenever two internal masses are degenerate.

Finally,

$$T^{ext} \equiv \sum_{i,j} \lambda_i \lambda_j \text{Im} \left\{ r_{ii}^{0*} \left[ \frac{r_{jj}^0}{|d_{ij}|^2} + \frac{m_j ((r_{ii}^0)^2 - (r_{jj}^0)^2)}{2d_{ii} d_{ij} d_{ji}} + \frac{r_{jj}^0}{d_{ii}} \left( \frac{1}{d_{ij}} + \frac{1}{d_{ji}} \right) \right] \right\}. \quad (5.22)$$

Although this expression is more involved, it vanishes whenever two external quarks masses are degenerate. This can be seen explicitly in a triangle construction for the analytic continuation to  $\omega + i\gamma$ , eq. (4.25), in the limit  $m \ll \gamma$ . Then,

$$d_{ij} \sim d_0 + O\left(\frac{m}{\gamma}\right) = -2(i\gamma + \omega) + \omega_R^0 + \omega_L^0, \quad (5.23)$$

leading to

$$T^{ext} \sim \frac{|d_0|^2 + 2\text{Re}(d_0^2)}{|d_0|^4} \sum_i \lambda_i \lambda_{i+1} (r_{i+1i+1}^0 r_{ii}^{0*} - r_{ii}^0 r_{i+1i+1}^{0*}), \quad (5.24)$$

where again the sum over  $i$  is modulo 3.  $T^{ext}$  is proportional to the oriented area of a triangle with vertices in the complex plane given by  $\lambda_i r_{ii}^0$ , Fig. 5-(b). When any two external quarks masses are degenerate, two of these points would coincide and the area would vanish. This shows that the GIM cancellation also works explicitly for external quark masses, as expected.

### 5.3 Results and Comparison with literature

We now give the numerical results we have obtained at  $O(\alpha_w^2)$  in the reflected baryonic flux, both for up external quarks (u,c,t) and downs (d,s,b). We have used the following values



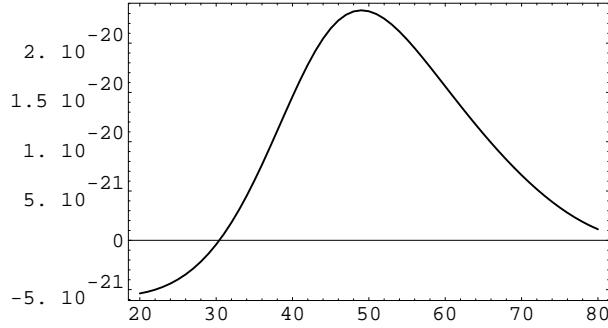


Figure 6: The dominant ( $O(\alpha_W^2)$ ) non-integrated CP asymmetry,  $\Delta_{CP}(\omega)$ , when mass effects are included inside thermal loops, as a function of the quasi-particle energy,  $\omega$ . The figure corresponds to charge 2/3 flavours.

for the masses in GeV,  $M_W = 50$ ,  $M_Z = 57$ ,  $m_d = 0.006$ ,  $m_s = 0.09$ ,  $m_b = 3.1$ ,  $m_u = 0.003$ ,  $m_c = 1.0$ ,  $m_t = 93.7$ . The couplings are  $\lambda_d = 1.2 \cdot 10^{-4}$ ,  $\lambda_s = 1.8 \cdot 10^{-3}$ ,  $\lambda_b = 6.2 \cdot 10^{-2}$ ,  $\lambda_u = 6.2 \cdot 10^{-5}$ ,  $\lambda_c = 2 \cdot 10^{-2}$  and  $\lambda_t = 1.88$ , and  $\alpha_s = 0.1$ ,  $\alpha_W = 0.035$ . Fig. (6) shows  $\Delta(\omega)$  for the ups (the dominant contribution). The result for the averaged ensemble asymmetry is,

$$\Delta_{CP}^{uct} = 1.6 \cdot 10^{-21}, \quad \Delta_{CP}^{dbs} = -3 \cdot 10^{-24}. \quad (5.25)$$

In both cases, we find that the asymmetry is dominated by the two heavier external quarks.

These results are several orders of magnitude in disagreement with the previous results obtained by Farrar and Shaposhnikov in ref. [11]. Their estimate is  $\Delta_{CP} \gtrsim 10^{-8}$  (see their eq. (10.3)). This tremendous discrepancy can fortunately be understood. There are mainly two important effects these authors did not consider. The first one, which explains the orders of magnitude difference, is that they disregard the effect of the damping rate in the scattering of the particles on the wall. In our calculation, however, it is an essential ingredient. The second difference, responsible for a small factor in the discrepancy, is due to the fact that they just considered the leading-T corrections in the self-energies. We have seen in the previous section that the subleading terms contain the dependence on the internal masses, essential for CP-violation. When they are neglected no  $O(\alpha_w^2)$  effect can appear, and the first contribution would loom at  $O(\alpha_w^3)$ .

In order to prove that these latter considerations are correct, we have reproduced their results, i.e. we have computed the CP-asymmetry just considering leading-T corrections in (5.4) and setting  $\gamma = 0$ . The result is shown in Fig. (7-a) and it is in complete agreement with the results in [11] (see Fig.5 in this reference). Improving their numerical calculation by the inclusion of the damping rate, gives the result shown in Fig. (7-b). The integrated asymmetry from fig (7-b) is  $\sim 4 \cdot 10^{-22}$ , to be compared to the result in fig (7-a) of [11],  $\sim 10^{-8}$ .

With or without the damping rate, it is also possible to work out an analytic expression at third order, from the perturbative calculation (5.12),(5.18). For  $\gamma = 0$ , the expected GIM cancellation appears, although there is no simple formula that explicitly shows them. On

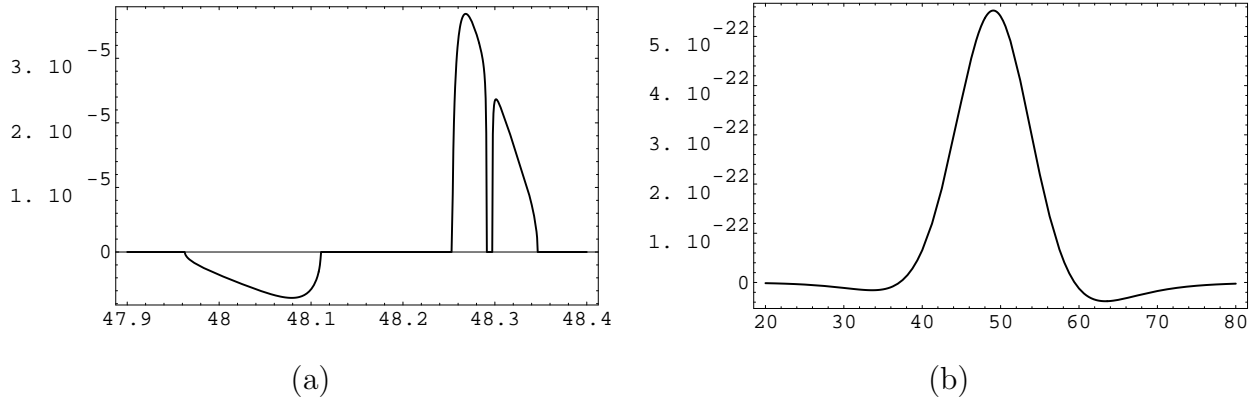


Figure 7: (a) shows the non-integrated CP asymmetry ( $\Delta_{CP}$ ) produced by down quarks in the narrow energy range which dominates for zero damping rate, when masses are neglected in the internal loop. (b) shows the dramatic effect of turning on the damping rate effects, in the same approximation.

the other hand, in the case  $\gamma \neq 0$  and in the limit  $m \ll \gamma$ <sup>23</sup>, the expression for the peak value of the asymmetry beautifully reduces to

$$\Delta_{CP}^{max} = \left[ \sqrt{\frac{3\pi}{2}} \frac{\alpha_W T}{32\sqrt{\alpha_s}} \right]^3 J \frac{(m_t^2 - m_c^2)(m_t^2 - m_u^2)(m_c^2 - m_u^2)}{M_W^6} \frac{(m_b^2 - m_s^2)(m_s^2 - m_d^2)(m_b^2 - m_d^2)}{(2\gamma)^9} \quad (5.26)$$

This was expected from naive order-of-magnitude arguments.

Finally, the results (5.25) show that non-leading effects in T give the main contribution to the asymmetry in the case of non-vanishing damping rate and, in contrast with [11], the up-sector dominates the asymmetry.

Very recently, Huet and Sather[28] have analyzed the problem. These authors state that they confirm our conclusions. As we had done in ref. [1], they stress that the damping rate is a source for quantum decoherence, and use as well an effective Dirac equation which takes it into account. They discuss a nice physical analogy with the microscopic theory of reflection of light. They do not use wave packets to solve the scattering problem, but spatially damped waves, as in our heuristic treatment at the beginning of Sect. 4.

## 5.4 Wall thickness.

Notice that the derivation in sect. 4 is totally independent of the shape of the function  $r(k)$ . The only requirement was a singularity structure limited to a cut in the region of total reflection. This is quite generic: only for very special wall shapes can other singularities be expected. For instance, when the wall is not monotonous, a pole with an imaginary part may express the decay of a quasi-bound state trapped in a potential well.

The thin wall approximation used in this paper is valid only for wall thickness  $l \ll 1/6\gamma$ , while perturbative estimates suggest  $l \geq .1\text{GeV}^{-1} \geq 1/6\gamma$ . The CP asymmetry, generated in

<sup>23</sup>This is valid for down external quarks, the case we considered

the presence of such more realistic walls, would be orders of magnitude below the thin wall estimate, eq. (5.25), reinforcing thus our conclusions, because a quasi-particle would then collide and lose coherence long before feeling a wall effect.

## 6 Conclusions.

At finite temperature a plasma is mainly an incoherent mixture of states. The scattering of quasi-quarks with thermal gluons induces a large damping rate,  $\gamma$ . Quantum coherence is only maintained between two inelastic scattering processes of this type. It is lost over spatial distances larger than  $\sim 1/6\gamma \sim (120 \text{ GeV})^{-1}$ , and over time scales larger than  $\sim 1/2\gamma \sim (40 \text{ GeV})^{-1}$ .

We have considered both an heuristic approach to quasi-quarks in terms of spatially damped waves, and a more physically sound one in terms of wave packets which incorporates the above mentioned characteristics of coherent mean free time and coherence length. With these tools, we have shown that coherent tree-level reflection of quasi-quarks hitting the bubble wall is suppressed for all flavours but the top, by a factor  $m/2\gamma$ . This effect might also be relevant in certain non-relativistic systems, e.g. in solid state physics. We have shown as well that a CP-violation reflection asymmetry appears already at order  $\alpha_W$  in amplitude, and it is suppressed by further powers of  $m/2\gamma$ . It fails to explain the baryon asymmetry by more than 12 orders of magnitude.

Any non-standard electroweak scenario for baryogenesis, where quantum coherence is required over distances and times larger than the above mentioned ones, is subject to the same flaw. In particular, “realistic” electroweak walls are thick, much larger than the coherence length. No (quark) coherence should be required through the whole wall thickness in a successful scenario. In a more positive view, it is worth to stress that promising candidate theories are those where CP violation is associated to the top and/or heavier flavours. Leptonic induced baryogenesis may also be safe.

## 7 Acknowledgements.

We acknowledge Tanguy Altherr, Luis Alvarez-Gaumé, Philippe Boucaud, Andy Cohen, Alvaro De Rújula, Savas Dimopoulos, Jean Marie Frère, Jean Ginibre, Gian Giudice, Jean-Pierre Leroy, Manolo Lozano, Jean-Yves Ollitreault, Anton Rebhan, Eric Sather, Dominique Schiff and Javier Vegas for many inspiring discussions. We are indebted to Nuria Rius for criticisms on the typescript. M.B. Gavela and P. Hernandez are indebted to ITP (Santa Barbara) for hospitality during the final period of this work, where their research was supported in part by the National Science Foundation under Grant No. PHY89-04035. C. Quimbay would like to thank COLCIENCIAS (Colombia) for financial support. P.H. acknowledges partial financial support from NSF-PHY92-18167 and the Milton Fund.

## A Proof of the simplified formula for the reflection probability.

This appendix develops a bound to the error introduced in eq. (4.24) when the integration  $\int_{-\infty}^0 dt_0$  in eq. (4.16) is replaced by  $\int_{-\infty}^{+\infty} dt_0$ . We derive an upper bound of  $u^{\dagger-\chi, \chi} \Psi_{ref}(0, 0; z_0, t_0, p_0, d, \chi)^{24}$ . A comparison of eqs. (4.9) and (4.15) shows that:

$$u^{\dagger-\chi, \chi} \Psi_{ref}(z, t; z_0, t_0, p_0, d, \chi) = \frac{1}{\sqrt{2\pi}} u^{\dagger-\chi, \chi} \int_{-\infty}^{+\infty} dp_{\chi} e^{-ip_{\chi} z} r_{\chi}(p_{\chi}) \tilde{\Psi}_{inc}(p_{\chi}, t; z_0, t_0, p_0, d, \chi) \quad (\text{A.1})$$

As  $p_{-\chi} = p_{\chi} + 3(\omega_{\chi}^0 - \omega_{-\chi}^0)$ , eq. (A.1) can be expressed as a convolution,

$$u^{\dagger-\chi, \chi} \Psi_{ref}(z, t; z_0, t_0, p_0, d, \chi) = u^{\dagger-\chi, \chi} \int dz_1 e^{-3i(\omega_{\chi}^0 - \omega_{-\chi}^0)z} \Psi_{inc}(z_1, t; z_0, t_0, p_0, d, \chi) \tilde{r}_{\chi}(z + z_1) \quad (\text{A.2})$$

where

$$\tilde{r}_{\chi}(z) = \frac{1}{\sqrt{2\pi}} \int e^{-ip_{\chi} z} r_{\chi}(p_{\chi}) \quad (\text{A.3})$$

The proof goes as follows. We first show that

$$\tilde{r}_{\chi}(z) = -i \sqrt{\frac{2}{\pi}} \theta(z) \int_{-\pi/2}^{+\pi/2} d\theta \cos(mz \sin \theta) \cos^2 \theta \quad (\text{A.4})$$

where  $m$  is the quark mass. This gives the bound

$$|\tilde{r}_{\chi}(z)| \leq \sqrt{\frac{\pi}{2}} m \theta(z). \quad (\text{A.5})$$

Next, this bound is inserted in eq. (A.2) and the final bound on the  $t_0 > 0$  contribution to the reflection probability in eq. (4.16) follows.

- Bound on  $\tilde{r}_{\chi}(z)$ .

The integral in (A.3) is computed using (4.5) and the analytic properties of  $r_{\chi}(p_{\chi})$ , explained after eq. (4.16). For  $z < 0$ , the contour can be closed on the upper half plane, with a vanishing result. Else, the cut has to be crossed with the result:

$$\begin{aligned} \int dp_{\chi} e^{-ip_{\chi} z} r_{\chi}(p_{\chi}) &= \theta(z) \int_{-m}^{+m} dp_{\chi} e^{-ip_{\chi} z} \left( \frac{m}{p_{\chi} + i\sqrt{m^2 - p_{\chi}^2}} - \frac{m}{p_{\chi} - i\sqrt{m^2 - p_{\chi}^2}} \right) \quad (\text{A.6}) \\ &= -\frac{im}{2} \int_{-\pi/2}^{+\pi/2} d\theta \cos(mz \sin \theta) \cos^2 \theta \end{aligned}$$

where a change of variables,  $p_{\chi} \rightarrow m \sin \theta$ , was performed. This completes the proof of eq. (A.4), and hence of eq. (A.5).

---

<sup>24</sup>The factor  $u^{\dagger-\chi, \chi}$  takes care of the spinor  $u_{-\chi, \chi}$  in  $\Psi_{ref}$ , so as to keep only the spatial dependence.

- Integrals on  $z_0$  and  $t_0 > 0$  for the incoming wave packet.

Before considering the effect of extending the integration on  $t_0$  in eq. (4.16) to  $+\infty$ , we discuss the simpler exercise of integrating the squared norm of the incoming wave  $\Psi_{inc}$ . The particle density  $\Xi$  in eq. (4.12) has been computed far from the wall in the unbroken region. For that reason, the integral on  $z_0$  extends to  $+\infty$ . Consider the same density close to the wall, i.e. for  $z = 0^-$  (and  $t = 0$  to be specific). Since only packets created in the unbroken region are relevant, we must now constrain the integral on  $z_0$  from  $-\infty$  to 0. This is the density of incoming quasi-particles hitting the wall,  $\Xi^{wall}$ :

$$\begin{aligned}\Xi^{wall} &= \int dp_0 dt_0 dz_0 \theta(-z_0) \theta(-t_0) |\Psi_{inc}^\chi(0, 0; z_0, t_0, p_0, d)|^2 N(z_0, t_0, p_0) \\ &< \frac{1}{2\gamma} \int dp_0 N(z_0, t_0, p_0) = \Xi.\end{aligned}\quad (\text{A.7})$$

where the inequality stems from the positivity of the integrand and the comparison with the integral in eq. (4.12). It is useful to notice that, if the integral over  $t_0$  in the first line of eq. (A.7) is extended to  $+\infty$ , we recover  $\Xi$  i.e. the same result as extending the integral over  $z_0$  to  $+\infty$ . Let us estimate the difference between  $\Xi^{wall}$  and  $\Xi$ , i.e. the effect of the integral over  $t_0 > 0$  on the incoming density. Afterwards we will extend the result to the reflected probability.

From the last line of eq. (4.10), it follows that

$$\begin{aligned}\Xi - \Xi^{wall} &= \frac{1}{d\pi^{1/2}} \int_{-\infty}^{+\infty} dp_0 \int_{-\infty}^{+\infty} dx \int_0^{3x} dt_0 e^{-\frac{x^2}{d^2} + 2\gamma t_0} N(z_0, t_0, p_0) \\ &= \frac{1}{d\pi^{1/2}} \int_{-\infty}^{+\infty} dp_0 n_F(\omega_\chi^0 + p_0/3, T) \int_{-\infty}^0 dx e^{-\frac{x^2}{d^2}} (e^{6\gamma x} - 1)\end{aligned}\quad (\text{A.8})$$

where the change variables to  $x = -z_0 + t_0/3$  was performed, and eq. (4.13) was used. Expanding to first order in  $3\gamma d$ , it follows that,

$$\Xi - \Xi^{wall} \simeq \frac{3\gamma d}{\pi^{1/2}} \Xi \ll \Xi \quad \text{if} \quad 3\gamma d \ll 1 \quad (\text{A.9})$$

where eq. (4.14) was used. The difference between  $\Xi$  and  $\Xi^{wall}$  consists in gaussian tails of size  $\sim d$ , small compared to the range of damping  $1/3\gamma$ . The same phenomenon is present in  $\Psi_{ref}$ , through  $\Psi_{inc}$ , which appears in the convolution (A.2).

- Integrals on  $z_0$  and  $t_0 > 0$  for the reflected wave packet.

From eqs. (A.2), (4.10) and (4.8), it follows

$$|\Psi_{ref}(0, 0; z_0, t_0, p_0, d, \chi)| \leq \frac{m}{2} \sqrt{\frac{1}{d\pi^{1/2}}} \int_0^\infty dz_1 e^{-\frac{(z_1 - z_0 + t_0/3)^2}{2d^2} + \gamma t_0} \quad (\text{A.10})$$

The contribution to the reflection probability, for  $t_0 > 0$ , is then bounded by

$$n_r^x(0, 0; t_0 > 0) \leq \frac{m^2}{2d\Xi\pi^{1/2}} \int_{-\infty}^{+\infty} dp_0 2\gamma n_F(\omega_\chi^0 + p_0/3) \times \int_0^\infty dz_1 dz_2 dz_0 dt_0 e^{-\frac{(z_1+z_0+t_0/3)^2+(z_2+z_0+t_0/3)^2}{2d^2}+2\gamma t_0} \quad (\text{A.11})$$

where a change of variable  $z_0 \rightarrow -z_0$  was performed. With the supplementary variables changes

$$z_1 + z_0 + t_0/3 = yd \cos \theta, \quad z_2 + z_0 + t_0/3 = yd \sin \theta, \quad z_0 + t_0/3 = xd, \quad t_0 = t_0, \quad (\text{A.12})$$

the integral over  $t_0$  leads to

$$\int_0^{3xd} dt_0 e^{2\gamma t_0} = \frac{1}{2\gamma} (e^{6\gamma xd} - 1) \simeq 3xd, \quad (\text{A.13})$$

while the integral on  $x$ , assuming  $\sin \theta \leq \cos \theta$ <sup>25</sup>, leads to

$$\int_0^{y \sin \theta} dx 3xd^2 = \frac{3d^2}{2} (y \sin \theta)^2 \quad (\text{A.14})$$

and, finally,

$$3d^4 \int_0^\infty dy y^3 e^{-\frac{y^2}{2}} \int_0^{\frac{\pi}{4}} d\theta \sin^2 \theta = 3d^4 \frac{\pi - 2}{4}. \quad (\text{A.15})$$

It follows that

$$n_r^x(z = 0, t = 0; t_0 > 0) \leq \frac{m^2 d^3 6\gamma}{\pi^{1/2}} \left( \frac{\pi - 2}{8} \right). \quad (\text{A.16})$$

When this result is compared to eq.(4.25),

$$n_r^x(0, 0) \simeq \frac{m^2}{\gamma\Xi} \quad (\text{A.17})$$

it is clear that the  $t > 0$  contribution is indeed suppressed,

$$\frac{n_r^x(0, 0; t_0 > 0)}{n_r^x(0, 0)} \sim (\gamma d)^2 (\Xi d) \ll 1 \quad (\text{A.18})$$

where we have used the fact that  $\Xi = O(g_s T)$  (a one-dimension density of quasiparticles with energy in the  $O(g_s T)$  range), and that it is easy to choose  $d$  such that the condition (4.27) is met simultaneously with  $(\gamma d)^2 (\Xi d) \ll 1$ . For example,  $1/d \sim g_s T$  satisfies all these criteria.

---

<sup>25</sup>By symmetry, the alternative sector,  $\sin \theta \geq \cos \theta$  gives the same contribution, leading to a factor of 2 in the final result.

## References

- [1] Standard Model CP-violation and Baryon asymmetry. M.B. Gavela, P. Hernandez, J. Orloff, and O.Pène, *Modern Physics Letters* 9A 795 (1994).
- [2] Standard Model CP-violation and Baryon asymmetry. Part I: Zero Temperature. M.B. Gavela, M. Lozano, J. Orloff, and O.Pène, CERN-TH.7263/94, LPTHE Orsay-94/48, HD-THEP-94-19, FAMNSE-12-94.
- [3] G. Steigman, *Ann. Rev. Astron. Astrophys.* 14 (1976) 339.
- [4] A.D. Sakharov *JETP Lett.* 6 (1967) 24.
- [5] A.D. Linde, *Phys. Lett.* 70B (1977) 306.
- [6] V.A. Kuzmin, V.A. Rubakov and M.E. Shaposhnikov, *Phys. Lett.* 155B (1985) 36.
- [7] For a recent review, see A.G. Cohen, D.B. Kaplan and A.E. Nelson, *Ann. Rev. Nucl. Part. Science* 43 (1993).
- [8] G. t'Hooft, *Phys. Rev. Lett.* 37 (1976) 8; *Phys. Rev. D* 14 (1976) 3432. N.S. Manton, *Phys. Rev. D* 28 (1983) 2019. F.R. Klinkhammer and N.S. Manton, *Phys. Rev. D* 30 (1984) 2212.
- [9] S. Dimopoulos and L. Susskind, *Phys. Rev. D* 18 (1978) 4500.
- [10] M. Kobayashi and T. Maskawa, *Prog. Theor. Phys.* 49 (1973) 652.
- [11] G.R. Farrar and M.E. Shaposhnikov, *Phys. Rev. Lett.* 70 (1993) 2833. G.R. Farrar and M.E. Shaposhnikov, CERN-TH.6732/93.
- [12] A. Cohen, D. Kaplan, and A. Nelson *Nucl.Phys.* B373 (1992) 453.
- [13] M.E. Shaposhnikov, *Nucl. Phys.* B 375(1992) 625.
- [14] M. Dine et al, *Phys. Lett.* 283B (1992) 319; *Phys. Rev. D* 46 (1992) 550.
- [15] L. McLerran, E. Mottola and M.E. Shaposhnikov, *Phys. Rev.* D 43 (1991) 2027.
- [16] G.F. Giudice and M.E. Shaposhnikov, *Phys. Lett.* 326B (1994) 118.
- [17] L. McLerran, B.-H.Liu and N. Turok, *Phys.Rev.* D 46 (1992) 2668.
- [18] C. Quimbay and S. Vargas, in preparation.
- [19] E. Braaten and R.D. Pisarski, *Phys.Rev.* D46 (1992) 1829 and references therein. R. Kobes, G. Kunstatter and K. Mak, *Phys. Rev. D* 45 (1992)4632.
- [20] V.V. Klimov, *Sov. J. Nucl. Phys.* 33 (1981) 934.
- [21] H.A. Weldon, *Phys.Rev.* D26 (1982) 2789.

- [22] E. Petitgirard, Z. Phys. C 54 (1992) 673.
- [23] See for example a definition and discussion of Wigner functions in R. Balescu, Equilibrium and Nonequilibrium Statistical Mechanics, John Wiley and sons, inc, New York, (1975).
- [24] D. Seibert, CERN-TH-7034/93.
- [25] M.B. Gavela, P. Hernandez and C. Quimbay, in preparation.
- [26] C. Jarlskog Phys. Rev. Lett. 55 (1985) 1039.
- [27] M.E. Shaposhnikov, JETP Letters 44 (1986) 445.
- [28] P. Huet and E. Sather, SLAC-PUB-6479 (1994).